Summer 6-28-2016

Modeling and Satellite Remote Sensing of the Meteorological Impacts of Irrigation During the 2012 Central Plains Drought

Clint Aegerter
University of Nebraska-Lincoln, clint.aegerter@huskers.unl.edu

MODELING AND SATELLITE REMOTE SENSING OF THE METEOROLOGICAL IMPACTS OF IRRIGATION DURING THE 2012 CENTRAL PLAINS DROUGHT

by

Clint J. Aegerter

A THESIS

Presented to the Faculty of

The Graduate College at the University of Nebraska

In Partial Fulfillment of Requirements

For the Degree of Master of Science

Major: Earth and Atmospheric Sciences

Under the Supervision of Professor Jun Wang

Lincoln, Nebraska

June, 2016

MODELING AND SATELLITE REMOTE SENSING OF THE METEOROLOGICAL IMPACTS OF IRRIGATION DURING THE 2012 CENTRAL PLAINS DROUGHT

Clint J. Aegerter, M.S.

University of Nebraska, 2016

Advisor: Jun Wang

As irrigation is increasingly needed for agricultural production, it is becoming progressively more important to understand not only how irrigation impacts water availability, but how the introduction of this water into the soil impacts weather and climate through land-atmosphere interactions. In the summer of 2012, the Central Plains of the United States experienced one of its most severe droughts on record. This study examines the meteorological impacts of irrigation during this drought through observations and model simulations using the Community Land Model (CLM) coupled to the Weather Research and Forecasting (WRF) model. A simple parameterization of irrigation processes is added into the WRF model. In addition to keeping soil moisture in irrigated areas at a minimum of 50% of soil moisture capacity, this irrigation scheme also has the following new features: (1) accurate representation of the spatial distribution of irrigation area in the study domain by using MODIS-based 250-m resolution land surface classification; and (2) improved representation of the time series of leaf area index (LAI) values derived from crop modeling and satellite observations in both irrigated and non-irrigated areas. Several numerical sensitivity experiments are conducted. The WRF-simulated temperature field when including soil moisture and LAI modification within the model is shown to be most consistent with ground and satellite observations, all indicating a 2-3 K decrease of temperature in irrigated areas compared to the control run.

Modification of leaf area index in irrigated and dryland areas led to smaller changes, with a 0.2 K temperature decrease in irrigated areas and up to a 0.5 K temperature increase in dryland areas. Furthermore, the increased soil moisture and modified leaf area index is shown to lead to increases in surface divergence, increases in surface pressure, and decreases in planetary boundary layer height over irrigated areas.

ACKNOWLEDGEMENTS

First, I would like to thank my advisor, Dr. Jun Wang, for creating an excellent learning environment within his research group. I was welcomed to the group as an undergraduate in 2013 and they have continued to help me learn and grow as a scientist throughout my time as a graduate student. While all members of the group have helped me in some way, I would especially like to thank Yun Yue and Dr. Cui Ge for assisting me with learning and troubleshooting the Weather Research and Forecasting (WRF) model, which was used extensively in my thesis.

I would also like to thank Dr. Robert Oglesby and Dr. Suat Irmak for serving as my committee members. Dr. Oglesby's expertise in modeling, as well as his climate modeling course, was very helpful as I designed and carried out my study. Dr. Irmak's expertise in biological systems engineering, a field outside of atmospheric sciences, provided several perspectives on irrigation modeling and crops, in general, that I would not have otherwise thought of. I would also like to thank Dr. Irmak for providing data from his Nebraska Water and Energy Flux Measurement, Modeling, and Research Network.

I also thank the NASA Nebraska Space Grant for financial support as I began this project and the University of Nebraska-Lincoln Department of Earth and Atmospheric Sciences for the continued aid in the form of a teaching assistantship and the meteorology computer lab system administrator job. I also appreciate the Holland Computing Center for providing the computing resources necessary for running WRF and the High Plains Regional Climate Center for providing data from their Automated Weather Data Network.

TABLE OF CONTENTS

LIST OF TABLES AND FIGURES

TABLES

FIGURES

1. Introduction

In the latest IPCC report (2013), the effect of land-use and land cover change is ranked as one of the largest uncertainties in global climate models. The addition of water to the soil through human activities such as irrigation, which is a common agriculture-related land-use, accelerates water cycles in the Earth system, thereby affecting the surface energy budget, regional climate, and crop yield (Adegoke et al. 2003, Evans and Zaitchik 2008). Worldwide, irrigated land area has increased from 40 million hectares in 1990 to more than 270 million hectares in 2000 and further increased by 11.49% to 301 million ha in 2010 (Siebert et al. 2005; Siebert et al. 2010). The total irrigated land in the United States has also increased in recent years, though more slowly than the global rate, from approximately 22.4 million ha in 2002 to 22.6 million ha in 2012, an increase of 0.89% (USDA 2004; USDA 2014). In a study by Maupin et al. (2014) it is estimated that irrigation accounted for 33% of the total water pumped in the United States in 2010, amounting to approximately 4.35×10^8 m^3 d^{-1} (115 billion gallons d^{-1}). As irrigation continues to become more prevalent, more water will be introduced into the atmosphere that would otherwise remain underground. Hence, it is important to understand how irrigation affects climate both at the global and regional scale.

This study aims to better understand the impacts of irrigation on regional climate in Nebraska during severe drought when irrigation would likely be used most. Irrigation in Nebraska is unique in many ways. Much of Nebraska has access to the Ogallala Aquifer (one of the largest aquifers in the world) which currently provides a sufficient amount of water to continue irrigation even during severe drought. When compared to other states, Nebraska was 7^{th} nationally in water pumped for irrigation, pumping $2.14 \times$

10^7 m^3 d^{-1} (5.66 billion gallons d^{-1}) in 2010, with approximately 76% being ground water, which is the 13th highest percentage of all states, but 2nd highest for states in the top 10 of total water pumped for irrigation (Maupin et al. 2014). Compared to the other states, Nebraska has experienced the largest areal increase of irrigated land in the past decade, from approximately 3.1 million ha in 2002 to 3.4 million ha in 2012, an increase of 9.68%, passing California to become the state with the largest total irrigated area (USDA 2004; USDA 2014).

Overall, irrigation is bringing a large amount of water to the surface—where it can possibly interact with the atmosphere—that would not otherwise be present. In 2012, the year examined in this study, the Central Plains of the United States (including Nebraska), experienced unprecedented drought since the ground-based data record began in late 1900s (Hoerling et al., 2014). This paper uses both numerical model and observation data (satellite and ground-based) to study irrigation's impacts on temperature and other atmospheric processes in 2012 in Nebraska. The rest of the paper is organized as follows: Section 2 contains a review of past studies on the impact of irrigation on climate, with a focus on the numerical modeling of the impacts, examining differences between this study and previous studies. Section 3 presents the datasets used in this study, while section 4 provides a description of the model and associated sensitivity experiments. Results and model validation are presented in section 5 and finally, section 6 contains the main conclusions of the study, as well as some ideas for future work.

2. Background and Motivation

Though irrigation's influence on regional climate has been examined by many past studies, its effects are still not completely understood with several (sometimes competing) impacts being illustrated in both observational studies and modeling studies. Early observational studies, as summarized in Sellers (1965) and further demonstrated by Bastable et al. (1993), showed very different diurnal energy budgets between vegetated and bare land surfaces. Recently, as documented by numerous studies and preliminary observational work, irrigation not only has a cooling effect during crop growing season in irrigated areas through its modulation of sensible and latent heat flux at the surface, but also can affect the regional and seasonal temperature through adding water vapor in the atmosphere and soil; the magnitude of these effects on temperature is found to be significant enough to mask or strengthen the warming effect from CO_2 at the regional scale (Adegoke et al. 2003; Bonfils and Lobell 2007; Skaggs and Irmak 2012; Kueppers et al. 2008; Lobell et al. 2008; Mahmood et al. 2004; Raddatz 2007). A modeling study by Sacks et al. (2009) showed that the cooling effect of irrigation in global and annual averages is negligible, but can be 0.5 K in many northern-hemispheric mid-latitude regions. Also using a global model, Puma and Cook (2010) showed that after the expansion of irrigation in North America, Europe, and Asia during the 20th century, a related cooling effect spread and intensified by the end of this time period. However, they also found that irrigation leads to boreal winter warming over North America and Asia in the latter part of the last century due to an enhanced greenhouse effect from increased water-vapor near the surface. In contrast, Cook et al. (2011) used a global model to study the effects of irrigation for future climate projections under the modern

greenhouse gas (GHG) scenario (year 2000) and increased (A1B) scenario (year 2050), and showed that the extent to which irrigation will continue to "mask" the warming from increased GHG forcing will be influenced by changes in the background evaporative regime, secondary irrigation effects such as clouds and precipitation, and human-related decisions and abilities to maintain (or increase) current irrigation rates.

Indeed, at the continental scale, the effects of irrigation on surface temperature and its secondary effects on clouds, precipitation, and atmospheric dynamics are found to be more significant. Saeed et al. (2009) presented an improvement in the simulation of the South Asian summer monsoon after considering irrigation processes in a regional climate model. Ozdogan et al. (2010) used a land surface model with reanalysis and satellite data and showed that irrigation resulted in a 12% increase in evapotranspiration when averaged over all irrigated areas in the continental United States during the 2003 growing season.

More comprehensive analysis has also been conducted to understand the effects of irrigation on climate at regional scale. Recently, Qian et al. (2013) showed that consideration of irrigation in the Southern Plains reduces the bias in WRF-simulated surface parameters (moisture, temperature, and fluxes), especially during dry years. They further found an irrigation-induced reduction of lifting condensation level and mixed-layer depth, and an increase of shallow clouds, although precipitation is only slightly increased and highly variable in space. Kueppers et al. (2007) showed an average decrease of 3.7 K and 7.5 K for August mean and maximum temperature over a 20-year (1981-2000) simulation in California where natural vegetation was converted to irrigated agriculture. Their model also estimated an irrigation-induced overall net temperature

decrease of 0.38 K for California in August. They further showed that this cooling stabilizes the atmosphere, and thus reduces the strength of westerly land-sea breeze by 20-40%, although no discernable change in clouds or precipitation was found. Their findings, however, contrast with Crook et al. (1996) and Pielke et al. (2001) who have shown that the irrigation-induced cooling at the surface can lead to increased convective inhibition (CIN) and, therefore, less convection. The cooling effect is also shown in the modeling work of Lawston et al. (2015) which examines the impacts of different irrigation methods (drip, sprinkler, and two flood methods with varying levels of water application aggressiveness) on 2-day weather forecasts in dry and wet precipitation regimes over the southern great plains. The sprinkler and more aggressive flood methods lead to 2 m temperature decreases (with respect to non-irrigated runs) near 5 K over and slightly downwind of irrigated areas, while the drip and less aggressive flood methods lead to 2 m temperature differences of around 1 to 2 K or less. Furthermore, Harding and Snyder (2012) note a decrease in precipitation over irrigated areas and an increase in precipitation over non-irrigated areas during drought years in their modeling study comparing irrigation's impacts on precipitation and the energy budget in the United States Great Plains during years with below normal, normal, and above normal precipitation. In general, they find that impacts are most amplified with increased irrigation fraction during drought years, which is also supported by Nebraska Water and Energy Flux Measurement, Modeling, and Research Network (NEBFLUX, Irmak 2010) data showing that the largest temperature differences between two adjacent fields (one irrigated, one rainfed) from 2008-2013 occurred during the 2012 Central Plains drought. They also note an overall increase in precipitation throughout the domain when

incorporating irrigation in simulations, regardless of the specific precipitation regime.

In summary, past research has shown that irrigation not only yields cooling at the surface, but can lead to changes in dynamics (e.g. circulations), clouds, and precipitation; these effects are more discernable at the regional scale and can vary by year and region, presumably due to the differences in large general circulations and regional climate. Building upon this previous work, this new study is unique in the following aspects.

First, our study region focuses on Nebraska and nearby northern Plains that have the largest area and amount of water used for irrigation, but relatively little research has been directed at studying irrigation effects on climate for this region. Some of the only past work with a similar regional focus was conducted by Adegoke et al. (2003, 2007), who found that consideration of irrigation overall improved the Regional Atmospheric Modeling System simulation of surface temperature in U.S. northern plains. However, while their model simulations are consistent with the observed temperature contrast between irrigated and non-irrigated areas in 1981-2000 (e.g., 3.7 K cooling), the simulations are only conducted for a half month, and it is unclear how such cooling may vary in severe drought year. The work of Lawston et al. (2015) also focused on portions of this region, but only on a relatively small area of southeast Nebraska and northeast Kansas. Their work also focused on 2-day forecasts, while this work focuses on simulations over an entire summer. The simulation domain used by Harding and Snyder (2012) also contains this region, but their work focused on impacts of irrigation throughout a domain which stretched over much of the United States Great Plains.

Second, by focusing on the 2012 severe drought, the most severe drought in this region since 1895 (Hoerling et al. 2013), this study will not only examine the surface

cooling due to irrigation, but also potentially improve the WRF model simulation through: (a) a more accurate spatial representation of irrigation area and (b) incorporation of crop modeling and surface observations within the land surface model to account for vegetation changes during the growing season in response to both irrigation and non-irrigation scenarios. Part (a) is motivated by the work of Maxwell et al. (2008); they showed that the U.S. Geological Survey 2001 National Land Cover Database (NLCD) underestimates crop land area by 1.4 million ha (1.8%) as compared to the U.S. Department of Agriculture 2002 Census of Agriculture, and hence, the irrigation area at the state level might be misrepresented in the default land-use database in WRF (which is shown to be the case in Nebraska). Part (b) is motivated by the fact that in much of the past modeling work, the only difference between the default, non-irrigated scenario and irrigation scenario is the addition of water into the soil (while land surface properties are kept the same). Additionally, this study also examines the "natural" scenario in which humans never plant crops, by changing of the vegetation canopy from cropland to native grassland. Overall, studying irrigation's impacts during drought provides insight into its "maximum" effects, as irrigation is used most during drought years. The gradient from relatively healthy crops in irrigated areas to stressed crops in nearby non-irrigated areas during severe drought also provides an opportunity to examine differences in these two areas when they are in nearly the same ambient environment. We detail our modeling approach for (a) and (b) in section 4.

3. Data

3.1 Moderate Resolution Imaging Spectroradiometer (MODIS)

Satellite datasets from MODIS aboard Terra for land surface temperature (LST), cloud fraction, and leaf area index (LAI) are used to study the characteristics of irrigated cropland during the 2012 Central Plains drought, a time when the irrigated area was quite apparent in these data. These satellite data are used to view some of the potential meteorological effects of irrigation (especially during the 2012 Central Plains drought) such as reduction in cloud fraction over irrigated areas. 2012 summer anomalies are calculated using the previous ten years as a reference. The references and spatial resolution for these datasets can be found in Table 1.

3.2 Ground-Based Observations

Ground-based 2 m air temperature data collected by the Automated Weather Data Network (AWDN) of the High Plains Regional Climate Center collected are used to evaluate the uncertainty in the analysis of satellite data, as well as the accuracy of the WRF simulations. Preliminary work (Wang et al. 2016) also used 2 m air temperature measured by the Nebraska Water and Energy Flux Measurement, Modeling, and Research Network (NEBFLUX) surface water vapor and energy flux towers (Irmak 2010). Air temperature data (from 2008 through 2013) from two NEBFLUX grassland sites were used in this preliminary work, with the two sites being geographically close to each other (within 1 km) and respectively located in rainfed (dryland) and irrigated settings. The temperature contrast of approximately 1-2 K between these two sites in 2012 therefore provided a baseline estimate of the irrigation effect on land surface

temperature (LST).

3.3 North American Regional Reanalysis (NARR)

Initial and boundary conditions for WRF are provided through the National Centers for Environmental Prediction's (NCEP) North American Regional Reanalysis (NARR) data (Earth System Research Laboratory 2015). The NARR dataset is "a long-term, consistent, high-resolution climate dataset for the North American domain" (Mesinger et al. 2006). The dataset has a spatial resolution of 32 km and a three-hourly temporal resolution spanning from 1979 to present.

3.4 MODIS Irrigated Agriculture Dataset (MIrAD)

The MODIS Irrigated Agriculture Dataset (MIrAD) is a gridded classification of irrigated agricultural lands across the continental U.S. at a spatial resolution of 250 m that makes use of the "National Land Cover Dataset, USDA Census of Agriculture irrigated area statistics, and annual maximum vegetation index calculated from MODIS imagery" (Brown et al. 2009; Pervez and Brown 2010; Brown and Pervez 2014). This dataset merged with the default WRF land-use dataset is used as the land-use dataset in this study. The MIrAD dataset represents areas of irrigation in Nebraska more accurately than the default land-use dataset in WRF (Figure 1) and has been shown to have relatively good (82%) pixel agreement with a Landsat-derived land-use dataset in Nebraska (Wardlow and Callahan 2014). Correctly representing areas of irrigation is vital when attempting to verify model output with observations.

4. Model and Methods

4.1 Weather Research and Forecasting (WRF) Model

The WRF model version 3.6.1, run at 12 km resolution, is used to simulate the potential effects of irrigation. The WRF model is a regional model used for both research and operational forecasting (Skamarock et al. 2008). Though originally designed as a mesoscale forecast model, WRF has been adapted for use in climate studies. This work seeks to more accurately represent the irrigation surface through the use of the Community Land Model (CLM) version 4.0 (Oleson et al. 2010; Lawrence et al. 2011). CLM also has a sophisticated surface albedo scheme, enhanced terrestrial water cycle, canopy interception and integration, runoff from the surface and subsurface, groundwater and water-table depth, soil water availability and soil evaporation, inclusion of carbon and nitrogen cycle dynamics that improves plant production and LAI, and frozen soil modifications. Aside from the land surface model, the physics and parameterization schemes used are the WRF defaults (Table 2).

4.2 Irrigation Area & Parameterization

By default, WRF uses land-use categories from United States Geological Survey (USGS) 24-category data. These data have a resolution of 1 km and are based on data collected by the Advanced Very High Resolution Radiometer (AVHRR) between April of 1992 and March of 1993 (USGS cited 2016). Therefore, this database is out of date, and as shown in Figure 1, it does not represent the irrigated areas present in 2012 which is necessary in order to be able to compare simulation results to observational data. To better represent irrigation in WRF, the USGS dataset are merged with MIrAD (Figure 1).

The merger process was carried out through requiring a certain number of MIrAD pixels within one WRF grid box to be classified as “Irrigated” in order to classify the land-use in that grid box as “Irrigated Cropland and Pasture” in WRF. For example, a threshold of 25% required 25% of the 250 m resolution MIrAD pixels contained within one WRF grid box (12 km resolution) to be classified as “Irrigated” in order to classify that entire WRF grid box as “Irrigated Cropland and Pasture.” In total, three different thresholds—25%, 50%, and 75%—were used in this merger process. Results of these three mergers were subjectively compared to the spatial distribution of irrigation well density and raw MIrAD data to determine which threshold to use in non-control WRF simulations. The 25% threshold seemed to match the best, even containing the “hole” of non-irrigated land (classified as “Dryland Cropland and Pasture”) present at the southeast edge of the large irrigated area in southeast Nebraska, so it is used as the land-use dataset in irrigated WRF runs.

Recent advancements in the complexity of LSMs have led to several attempts to accurately parameterize irrigation. One of the most popular ways to parameterize irrigation is to simply add soil moisture at a specified time interval, or possibly keep soil moisture constant, in irrigated areas (Adegoke et al. 2003; Jiang et al. 2014; Kueppers et al. 2007; Kueppers and Snyder 2011; Zaitchik et al. 2005). Other methods include adding water as precipitation in irrigated areas (Ozdogan et al. 2010) and increasing evapotranspiration (ET) or vapor flux over irrigated areas (Douglas et al. 2006; Segal et al. 1988; Evans and Zaitchik 2008).

Lawston et al. (2015) studied three of the main parameterizations of irrigation (drip, flood, and sprinkler) by using 5-year spinups of NASA’s Land Information System

(LIS) to initialize 2-day WRF forecasts at 1 km resolution over the Great Plains of the United States. The “drip” method was implemented through adding the exact amount of water required to avoid soil moisture stress (calculated by finding the difference between canopy resistance using current soil moisture and canopy resistance assuming no soil moisture stress, and then finding these resulting ET values). Two “flood” methods were implemented through adding enough water to saturate the root zone if the soil moisture in this area fell below 25% above the wilting point (“Flood25”) or 75% of the wilting point (“Flood75”). Finally, the “sprinkler” method added water as precipitation at a user-specified rate (5 mm h^{-1} in the study) when root zone moisture availability (RZMA) fell below 10% above the stress point until RZMA reached 80% of the soil moisture capacity.

For this study, additional moisture from irrigation is parameterized through increasing soil moisture in irrigated areas in all layers (ranging from 0 to 3.433 m) to 50% of soil moisture capacity if this area falls below 50% of soil moisture capacity (where soil moisture capacity is determined by porosity of the soil in a given area). Therefore, soil moisture in irrigated areas can be greater than 50% of soil moisture capacity during precipitation events. Though many previous studies force soil moisture to saturation (i.e. 100% of soil moisture capacity), 50% is used in this study as entire fields (much less entire 12 km grid squares) are not saturated instantaneously through irrigation, because center pivot irrigation, which is the most common irrigation method (87.7%) in Nebraska, can take nearly two days to water an entire field (USDA 2014). Though not as complex as other irrigation parameterizations, this simple-to-implement method (combined with modified LAI values discussed in section 4.3) is the first step toward future studies to implement more realistic irrigation schemes. Indeed, no consensus can

be found in literature on how irrigation should be added in the land surface model. Keeping a simple and consistent irrigation parametrization facilitates the sensitivity analysis of various changes to surface representation in the modeling of irrigation impacts.

4.3 Temporal Variation of LAI

One of the main phenological impacts of irrigation is usually the increase of LAI relative to non-irrigated plants, especially during drought. MODIS data provide an excellent way to monitor these changes in LAI throughout a given growing season (Figure 2). In a normal precipitation year, such as 2008, croplands show a distinct seasonal cycle of greenness (in terms of green LAI): no discernable greenness from space in early June (Figure 2a), some greenness (with LAI value of 2) in late June and early July (Figure 2c), maximal greenness (with LAI value of up to 4-5) in late July and early August (Figure 2e), and then decrease of greenness (with LAI value less than 4) in late August and early September (Figure 2g). The “normal” year of 2008 was selected by finding the smallest precipitation departure from normal in Nebraska from 2002 through 2011 (NCEI cited 2016). Consequently, the dryland cropland in northeastern Nebraska is much more difficult to distinguish from the irrigated area in southeast Nebraska when simply looking at LAI values in 2008 (Figure 2e and Figure 2g).

However, in the drought year of 2012, while the greenness of crops indeed started earlier (Figure 2d, when compared to 2008, Figure 2c), the dryland cropland (much of northeastern Nebraska) dies off during the peak of growing season and the irrigated area in southeast Nebraska remains relatively healthy (as revealed from comparison between

Figure 2f for 2012 and Figure 2e for 2008).

Since changes in LAI occur based on the soil and precipitation conditions, this response is considered by changing the prescribed LAI time series in the simulation. Two approaches are used, based on satellite-based observation (CLM default), and simulation of crop models (Hybrid Maize crop model, Yang et al. 2004) for various meteorological conditions in 2012. The Hybrid Maize model simulates corn growth under irrigated and non-irrigated conditions based on the following daily weather variables: maximum air temperature, minimum air temperature, total solar radiation, rainfall, potential evapotranspiration, and relative humidity. The Hybrid Maize model is well-validated through comparison of its LAI output, along with the output of two other crop models (INTERCOM (Kropff and van Laar 1993) and CERES-Maize (Jones and Kiniry 1986)), with observations from three fields with varying plant density in Lincoln, Nebraska for the years 1999 through 2001. Overall, Hybrid Maize showed an average modeling efficiency (similar to r^2) of 0.903 over the three years, while INTERCOM and CERES-Maize showed average modeling efficiencies of 0.703 and 0.74, respectively, though all models tended to under-predict maximum LAI values (Yang et al. 2004). While much of the irrigated area in Nebraska contains both corn and soybeans, the LAI values for corn from the Hybrid Maize model can be representative to both corn and soybeans, assuming the crops are planted at a similar time (soybeans are commonly planted immediately after corn in Nebraska).

Figure 3 illustrates the differences in LAI values used by default in CLM, those simulated by the Hybrid Maize model, and those detected via MODIS. The MODIS LAI values shown in Figure 3 are 8-day averages within three areas—one irrigated and two

non-irrigated—which are shown in Figure 3b. The areas were selected based on land-use categories in the 25% merged land-use dataset used in several of the WRF simulations in this study. The irrigated area is within the main area of irrigation in southeast Nebraska. The non-irrigated area in Nebraska is a small, non-irrigated area on the southeast edge of the main irrigated area in Nebraska. Because this area is essentially surrounded by the main area of irrigation in Nebraska, it provides an almost ideal area for comparison with the irrigated area, as both areas experience nearly the same ambient meteorological conditions. However, due to its small areal extent, the non-irrigated area contains very few MODIS pixels, so the LAI averages for another non-irrigated area (located in north central Iowa) are also calculated. Because the default CLM irrigated (dryland) LAI is weighted as 85% irrigated (dryland) cropland and 15% urban area (LAI of 0), the Hybrid Maize data are weighted the same for a more direct comparison.

Although the default CLM values seem to compare somewhat close to those observed by MODIS, it should be noted that these MODIS observations are from a drought year (2012), so the actual values are likely greater than those used by CLM. Also, by default, CLM uses the same LAI values for both irrigated and dryland areas, which is clearly not the case in a drought year such as 2012. Regardless, both MODIS observations and crop models consistently show that irrigated crops (purple color shaded and blue line in Figure 3a) have larger LAI values and a longer growing season (before LAI decrease to 1) than their counterparts of non-irrigated dryland crops (pink color shaded and red line in Figure 3a). In addition, while the Hybrid Maize model overall provides larger LAI values (by 1) in the peak of growing season than corresponding satellite observations (regardless of irrigated land or dry land), both satellite and Hybrid

Maize model simulations show that LAI values over irrigated area are larger (also by 1) than those over dryland cropland. The CLM-default time series of LAI appears (black line in Figure 3a) is not consistent with either satellite-based or crop modeling analysis, as it shows a growing season with a starting date in early April and ending data in late October. We will use the LAI time series from Hybrid Maize model to replace the default LAI time series in WRF and assess the impact of this replacement in the simulation.

4.4 Numerical Experiment Design

This study analyzes output from seven WRF simulations, as summarized in Table 3. (1) WRF-DF (default) is simply WRF version 3.6.1 as downloaded (with default land-use and the default satellite-derived leaf area values in CLM). (2) WRF-DF-50S is the same as WRF-DF, but also makes use of an irrigation parameterization scheme which increases soil moisture to 50% of soil moisture capacity if soil moisture falls below 50% of soil moisture capacity. (3) WRF-Ctrl serves as the control simulation and is the same as WRF-DF, but makes use of the 25% threshold USGS/MIrAD merged land-use dataset as discussed in section 4.2. This merged land-use dataset is also used in the three following simulations. (4) WRF-DS-HLAI (default soil moisture, Hybrid Maize LAI) once again uses default soil moisture, but makes use of Hybrid Maize model simulated LAI values for irrigated and non-irrigated cropland. (5) WRF-50S-DLAI (50% soil moisture, default LAI) and (6) WRF-50S-HLAI (50% soil moisture, Hybrid Maize LAI) use the default LAI and Hybrid Maize model simulated LAI values, respectively, but also make use of the irrigation parameterization scheme used in (2) WRF-DF-50S. Finally, (7) WRF-NoIrri makes use of a land-use dataset in which all irrigated cropland in Nebraska

and immediately surrounding areas is converted to grassland. Soil moisture and LAI values are not modified in this simulation. This is meant to simulate a hypothetical situation in which humans are not able to grow crops in irrigated areas (i.e. humans only planted crops in those areas because groundwater for irrigation was available). Unless otherwise noted, the WRF simulation results are averaged at 18 UTC in order for a more direct comparison with data collected from Terra-MODIS, as 18 UTC is the approximate overpass time of Terra over Nebraska.

5. Impacts on Temperature

5.1 Impact from Additional Soil Moisture

WRF simulations of summer-averaged 2 m temperature (T_{2m}) at 18 UTC in Nebraska show temperature decreases throughout the state (compared to WRF-DF and WRF-Ctrl) when incorporating the "50S" irrigation parameterization (Figure 4). Comparison between WRF-DF-50S (Figure 4b) with WRF-DF (Figure 4a) shows a 1 K decrease of T_{2m} due to irrigation immediately over the default land-use irrigated area located in southwest Nebraska (Figure 4c). Though the default irrigation area is not in the correct location, the decrease of T_{2m} does illustrate that CLM physics are operating as expected (i.e. more soil moisture leading to more latent heating/less sensible heating and, therefore, cooler temperatures). Simply introducing an irrigated area that is more spatially accurate (WRF-Ctrl), as shown in Figure 4d, does not lead to any noteworthy temperature difference in Nebraska as a whole. However, combining the modified land-use with the 50S irrigation parameterization (WRF-50S-DLAI, Figure 4e) leads to nearly a 2 K temperature decrease over the most densely irrigated area in southeast Nebraska (Figure 4f); the geographical distribution of this T_{2m} decrease is in good agreement with the Terra MODIS LST anomalies (Figure 4i) which are between 0 K and 2 K for a10-year (2002-2011) average of LST (Figure 4g). Furthermore, comparison of these simulations to MODIS LST unsurprisingly shows that among all four numerical experiment results in Figure 4, WRF-50S-DLAI (Figure 4e) is the closest to MODIS LST in the irrigated areas (Figure 4h) in terms of spatial distribution of temperature. Note that because MODIS's LST is a retrieval parameter and reflects the radiation emitted from both canopy and land surface itself, there is no WRF parameter that can be directly quantitatively compared

with MODIS LST for all areas. We use T_{2m} here because that is the parameter often measured by weather stations and thus can be evaluated with these observations.

5.2 Impact from Leaf Area Index Modification

Modification of LAI in CLM to use values simulated by the Hybrid Maize model leads to a similar distribution of T_{2m} in Nebraska as WRF-Ctrl simulated (Figure 5a and Figure 4d). Overall, modified LAI has a much smaller impact on temperature (Figure 5f) than adding soil moisture to simulate irrigation (Figure 4f). Despite the relatively small impact on temperature, one unique aspect of the modified LAI is that while all other simulations led to cooler temperatures throughout Nebraska, WRF-DS-HLAI actually led to warming in some areas. Small T_{2m} increases of up to 0.5 K in a few spots can be seen in dryland areas in eastern Nebraska—likely due to crops in the dryland areas beginning to grow later and dying earlier than in the WRF-Ctrl run (as seen in Figure 3a)—though the magnitude of these temperature increases is not that significant (Figure 5f). When combining the addition of soil moisture to the modification of LAI (Figure 5b), the changes in 2 m temperature are much more significant with small areas of temperature decreases in southeast Nebraska over 2.5 K when compared to WRF-Ctrl (Figure 5c). Comparing WRF-50S-HLAI to WRF-DS-HLAI is another way to quantify the impact of adding soil moisture; this comparison shows a temperature decrease greater than 2 K (Figure 5d). Finally, the comparison of WRF-50S-HLAI to WRF-50S-DLAI shows a temperature decrease near 0.5 K through much of the irrigated areas (Figure 5e). This particular decrease is interesting, as simply changing the LAI in 50S runs leads to a larger temperature decrease than doing the same in non-50S runs. One hypothesis explaining

this is that with larger leaves, plants will transpire more, leading to increased evapotranspiration. Because the soil moisture is increased in the 50S runs, there is more soil moisture available for evapotranspiration and thus, a greater cooling effect is observed.

5.3 Impact of No Irrigated Cropland

As previously mentioned, the WRF-NoIrri run is meant to simulate what would happen if farmers never planted crops in the present-day irrigated areas and instead these areas were grasslands, the likely "native" land-use in these areas. This could also be a hypothetical scenario in which the groundwater resources in Nebraska become too depleted to sustain irrigation practices. No major changes with respect to WRF-Ctrl in T_{2m} distribution are observed in the WRF-NoIrri simulation (Figure 6a). When compared to WRF-Ctrl, the grassland substitution leads to a 1 K cooling effect over the area (Figure 6b). This further shows the model's inability to handle irrigated cropland using the default WRF setup with land-use changed, as it would be expected that grasslands would be warmer than irrigated cropland. In contrast, and as expected, when comparing the WRF-NoIrri simulation to WRF-50S-HLAI, higher T_{2m} values are present where irrigated cropland was replaced with grasslands (Figure 6c). Most of this temperature difference can likely be attributed to much lower soil moisture values in the WRF-NoIrri run, though the grassland land-use in CLM also has lower LAI values compared to the Hybrid Maize values used in WRF-50S-HLAI (peak of 2.38 vs. peak of 4.09, respectively). LAI values for grassland CLM values are actually quite similar during the peak of the growing season, as default CLM irrigated LAI peaks at 2.55.

5.4 Impact Above the Surface

While the impacts of irrigation on T_{2m} are readily visible in the previously discussed figures, it is important to examine how far this temperature impact extends vertically. To do this, the temperature field was analyzed at the 925, 850, 700, 500, 400, 300, 200, 150, and 100 hPa levels for each run. The highest level at which any definitive pattern was visible was at 850 hPa, which is illustrated in Figure 7. The simulated 18 UTC average temperature at 850 hPa (T_{850}) from WRF-Ctrl is shown in Figure 7a. Results show the expected pattern of an increase in T_{850} to the west, as elevation increases and 850 hPa becomes closer to the surface (note the white areas in the Nebraska panhandle are locations in which the surface pressure is less than 850 hPa). Similar to impacts on T_{2m}, all simulations show a cooling effect at 850 hPa throughout most of Nebraska. WRF-DS-HLAI has the smallest impact on temperatures, with maximum T_{850} decreases near 0.20 K (Figure 7b). WRF-50S-DLAI and WRF-50S-HLAI once again exhibit the largest temperature decreases, with maximum decreases over 0.60 K, and WRF-50S-HLAI showing a slightly larger area experiencing the maximum decrease (Figure 7c and Figure 7d). The WRF-NoIrri simulation also shows a cooling effect on T_{850}, much like it showed a cooling impact on T_{2m}, with maximum decreases near 0.40 K (Figure 7e). While these temperature impacts are relatively small in magnitude, they are systematic and persistently follow the irrigated areas in the WRF-50S-DLAI and WRF-50S-HLAI simulations. Examination of simulated temperatures at 700 hPa also shows a temperature decrease throughout most of Nebraska, though no obvious pattern is seen with regards to its spatial correlation with the irrigated area, so it is not shown. Therefore,

the vertical extent of irrigation's impacts on temperature likely ends between 850 hPa and 700 hPa, which correspond to standard atmosphere heights of 1500 m and 3000 m, respectively. This cooling aloft, though small in magnitude, would lead to an increase in convective available potential energy, as well as smaller dewpoint depressions, which would in turn favor the presence of clouds.

5.5 Model Evaluation

In general, incorporating an irrigation parameterization in CLM leads to a decrease of near-surface temperatures over irrigated areas. To determine if the magnitude of this cooling effect simulated by the model is at least somewhat realistic, simulated T_{2m} is compared to AWDN-observed T_{2m} (Figure 8). This analysis shows that the WRF-Ctrl simulated summer-averaged T_{2m} at 18 UTC was over 6 K warmer than observations in many irrigated locations (Figure 8b). Modifying LAI in the WRF-DS-HLAI run does not produce much of a change from the WRF-Ctrl run (Figure 8c). However, adding soil moisture reduces the temperature difference by 1-3 K in irrigated areas (Figure 8d). Combining the additional soil moisture with modified LAI reduces the temperature difference by another 1 K in some locations (Figure 8e). WRF-NoIrri temperature comparisons with AWDN are included in Figure 8f for completeness.

Figure 9 provides another way of illustrating improvements made in the simulation through the addition of soil moisture and modification of LAI by comparing average observed T_{2m} by AWDN to corresponding WRF grid squares by time of day. It is readily apparent that simulated vs. observational T_{2m} differences are greatest during the daytime/peak heating, while simulations were closer to observations at night. This diurnal

temperature difference could be due to the rather conservative nature of the soil moisture modification, leading to a larger difference during the day. Also, with the effects of irrigation being less at night (less evaporative cooling) irrigated areas will exhibit similar temperature characteristics to nearby non-irrigated areas (cropland and otherwise), which are where AWDN stations are located. This leads to a small temperature difference at night. For each plot, WRF averages were calculated using the WRF grid box that contained an AWDN station. Figure 9a shows averages for all AWDN stations and the corresponding WRF grid boxes. Figure 9b calculates the averages using only AWDN stations falling within WRF grid boxes classified as Irrigated Cropland and Pasture and Figure 9c is similar, but for WRF grid boxes classified as Dryland Cropland and Pasture. The land-use classification of each station is illustrated in Figure 8a. Figure 9 illustrates that the greatest improvement is made for irrigated areas, but only a 2-3 K cooling is experienced when using WRF-50S-HLAI vs. WRF-Ctrl. On average, the irrigated locations containing AWDN observations in the WRF-50S-HLAI simulation are still approximately 4 K too warm at 21 UTC, the time of maximum T_{2m}. Table 4 provides hourly average error for each model run and each land-use.

6. Secondary Impacts

One other potential meteorological impact of irrigation is a possible reduction in cloud fraction over irrigated areas. Previous work using monthly MODIS cloud fraction data showed a negative cloud fraction anomaly in Nebraska in 2012 (decrease in clouds compared to the average of the previous ten years), as would be expected during a drought, though the largest reduction was over the heavily irrigated area in southeast Nebraska (Wang et al. 2016, Figure 10a). A similar pattern was also shown when 5 km resolution daily level 2 MODIS cloud fraction granules were re-gridded to 0.25°×0.25° (Figure 10b). Though the largest decrease in cloud fraction was not located directly over the area in southeast Nebraska that is the most densely irrigated, a local minimum in cloud fraction anomaly (large decrease in cloud fraction) does exist just north of this area, which is also irrigated (though not as heavily). One potential hypothesis for this is the development of a sea-breeze-like circulation in which air rises over the warmer, non-irrigated areas and subsides over the cooler, irrigated areas, leading to less cloud cover in the irrigated areas. Similar circulations are described by Ookouchi et al. (1984).

One way to test the plausibility of this hypothesis is to examine simulated divergence, as subsidence over irrigated areas would lead to surface divergence. In general, simulation results show surface divergence over irrigated areas and convergence, or less divergence in some cases, over non-irrigated areas (Figure 11). When additional soil moisture is added in WRF, irrigated areas experience enhanced divergence, relative to non-50S simulations. However, the modification of LAI leads to different results depending on the presence of added soil moisture. The WRF-Ctrl simulation averaged at 18 UTC shows no discernible pattern in Nebraska, other than a large convergent zone in

northwest Nebraska and a small divergent zone in the panhandle (Figure 11a). Simply modifying the LAI of WRF-Ctrl leads to very little change throughout Nebraska (Figure 11b). Figure 11c and Figure 11d show that additional soil moisture leads to more surface divergence over irrigated areas. Figure 11e and Figure 11f show difference plots between WRF-DS-HLAI/WRF-Ctrl and WRF-50S-HLAI/WRF-Ctrl. In these plots, only areas found to be statistically significant at a 95% confidence level using a two-tailed, paired *t* test are plotted. Clearly, WRF-DS-HLAI has very little significant change from WRF-Ctrl. In contrast, WRF-50S-HLAI exhibits several statistically significant areas, including the area of divergence in the Nebraska panhandle, which is present in WRF-Ctrl, but Figure 11f illustrates just how much larger the divergence becomes when adding soil moisture and changing LAI. Also present is a relatively large area of increased surface divergence in east central Nebraska; this area corresponds quite well to the aforementioned local minimum in cloud fraction anomaly.

Another hypothesis related to wind flow over irrigated and non-irrigated areas is that warmer temperatures over non-irrigated areas will lead to enhanced mixing and, therefore, wind direction will be closer to that of the wind aloft as momentum is mixed downwards. In contrast, cooler temperatures over irrigated areas promote less mixing, and, therefore, the wind direction will be farther away from that of the wind aloft when compared to the wind direction over non-irrigated areas. Depending on the location of irrigated areas relative to non-irrigated areas, this could lead to enhanced convergence at the interface of these two areas. This hypothesis is illustrated in Figure 12. A narrow band of increased convergence in southwest Nebraska is visible in Figure 10f. This band is located just to the west of the main area of irrigation in Nebraska, which would support

the hypothesis, but is also to the east of another smaller area of irrigation and increased divergence. Therefore, this area could simply be the convergence zone that would have to form in between two areas of divergence. A similar area exists in south central Nebraska, with increased convergence in between two areas of irrigation and increased divergence.

Another secondary impact of irrigation that is readily visible in the WRF simulations is a decrease in planetary boundary layer height (H_{PBL}). Figure 13a illustrates the 18 UTC average H_{PBL} from the WRF-Ctrl simulation. Overall, H_{PBL} tends to increase moving west throughout Nebraska. Once again, the WRF-DS-HLAI simulation shows very little change relative to the WRF-Ctrl simulation, as very few statistically significant areas show up (Figure 13b). Large decreases in H_{PBL} near 500 m corresponding well with irrigated areas are simulated by WRF-50S-DLAI and WRF-50S-HLAI (Figure 13c and Figure 13d). WRF-NoIrri also shows a statistically significant decrease in H_{PBL} near 200 m in the areas converted to grasslands (Figure 13e). None of these results are surprising, as the decreases in H_{PBL} correspond well to decreases in temperature.

It is also shown that WRF-50S runs lead to an increase in surface pressure over the irrigated areas in Nebraska (Figure 14). The general pattern in surface pressure simulated by WRF-Ctrl shows the expected decrease moving west through Nebraska as terrain elevation increases (Figure 14a). As has been the case for nearly all variables examined thus far, WRF-DS-HLAI simulates almost no statistically significant change relative to WRF-Ctrl (Figure 14b). WRF-50S-DLAI, WRF-50S-HLAI, and WRF-NoIrri simulate statistically significant, though small in magnitude, pressure increases of approximately 0.30, 0.40, and 0.10 hPa, respectively (Figure 14c, Figure 14d, and Figure 14e). The center of the higher pressures corresponds quite well to the largest decrease in

cloud fraction seen in the re-gridded level 2 MODIS cloud fraction data in Figure 10b.

Finally, this study briefly examines the potential impacts of irrigation on precipitation. If the sea-breeze circulation does occur, this should ideally in turn lead to a decrease in precipitation over irrigated areas. Also, if there are enhanced areas of convergence along boundaries between irrigated and non-irrigated areas, these areas (or possibly areas downwind) could receive more precipitation. Previous studies on this subject show contrasting results with some indicating an increase in precipitation occurs downwind of irrigated areas (DeAngelis et al. 2010) while others find an increase in precipitation directly over irrigated areas (Harding and Snyder 2012). This study finds no significant pattern changes in precipitation from run to run.

7. Summary and Conclusions

Both modeling and observational studies show that irrigation can have a significant impact on regional weather and climate. Through model simulations, as well as both ground-based and satellite-based observations, this study attempted to understand the impact of irrigation on weather and climate during a time of severe drought in Nebraska. A parameterization scheme for irrigation was added into WRF. Though simple, this scheme has several aspects:

(1) Irrigation area must be spatially represented accurately. To accomplish this, the MIrAD dataset is merged with the default WRF land-use dataset and compared to registered well data to determine a suitable representation of irrigation land-use.

(2) Soil moisture must be added to represent the direct effects of irrigation. In this study, soil moisture in irrigated areas is kept at a minimum of 50% of soil moisture capacity. Compared to many previous studies which saturate the soil in irrigated areas, this is a rather conservative approach. However, center pivot irrigation, which is the main type of irrigation used in Nebraska, does not instantaneously saturate the soil in an entire field, and therefore, simulating irrigation by saturating entire WRF grid cells is an inaccurate representation.

(3) The physical response of plants to irrigation, such as increased LAI in irrigated areas, must be accounted for in the land surface model. While this is technically accounted for in past studies, as most land surface models have a default satellite-derived time series of LAI values for different land-uses, no study addresses the issue that these time series are not necessarily applicable in all simulation time periods. For example, during drought, crops that are not irrigated will likely wilt and/or die during the growing

season, leading to reduced LAI values in these areas. However, because the LAI values are not dynamically-simulated, these plants remain healthy in model simulations during drought. To address this, this study uses simulated 2012 LAI values for irrigated and dryland cropland from the Hybrid Maize crop model. These values account for the early wilting and death of non-irrigated crops and also give a higher peak LAI value for both irrigated and dryland crops, allowing for examination of the model's sensitivity to these changes.

This parameterization scheme enabled us to conduct a series of numerical experiments to simulate the model sensitivity to these different aspects of the parameterization. We found that inclusion of all three parameterization aspects led to simulation results most consistent with satellite and ground-based temperature observations. Simply changing the land-use dataset from the default WRF land-use had nearly no impact on simulated temperature. Combining the modified land-use with the modified LAI time series also led to very little change in simulated temperatures, with temperature decreases in irrigated areas of at most 0.25 K in irrigated areas relative to WRF-Ctrl. The modified LAI values also led to an increase in temperatures of a similar magnitude in dryland areas. The introduction of additional soil moisture had a much larger impact on simulated temperatures than any other aspect of the parameterization scheme, leading to a temperature decrease of 1-2 K in irrigated areas relative to WRF-Ctrl. Incorporating the modified leaf are index time series led to an additional 0.5-1 K temperature decrease in these areas.

Several secondary impacts of irrigation were also examined. We found that incorporating irrigation led to increased surface pressure in irrigated areas. Along with

this pressure increase was an increase in surface divergence, supporting the hypothesis of a circulation occurring in which subsidence takes place over irrigated areas. A more divergent and anticyclonic pattern is also seen in the main irrigated area in southeast Nebraska when plotting 10 m wind difference between WRF-50S-HLAI and WRF-Ctrl. Finally, the planetary boundary layer height over irrigated areas was found to decrease by nearly 500 m.

In addition to the irrigation parameterizations, a final WRF run was conducted in which the irrigated areas in Nebraska were replaced with grasslands. This was to simulate the hypothetical situation such as one in which farmers cannot grow crops in these areas because there is no groundwater with which to irrigate. This simulation was warmer than the WRF-50S-HLAI simulation by just over 1 K in the newly-introduced grassland areas. These same areas were also cooler than the corresponding irrigated area in WRF-Ctrl, though by less than 1 K. It is likely that modification of the LAI time series for grasslands would lead to more accurate results, as grasslands were shown via MODIS data to have LAI values between 0 and 1 during the 2012 drought. Overall, this simulation served as another method of examining how humans have impacted weather and climate, which will continue to be an important issue moving forward.

References

Adegoke, J. O., R. A. Pielke, J. Eastman, R. Mahmood, and K.G. Hubbard, 2003: Impact of irrigation on midsummer surface fluxes and temperature under dry synoptic conditions: A regional atmospheric model study of the U.S. High Plains. *Mon. Wea. Rev.*, **131**, 556–564.

Bastable, H. G., J. W. Shuttleworth, R. L. G. Dallarosa, G. Fisch, and C. A. Nobre, 1993: Observations of climate, albedo and surface radiation over cleared and undisturbed Amazonian forest. *Int. J. Climatol.*, 13, 783–796.

Bonfils, C. and D. Lobell, 2007: Empirical evidence for a recent slowdown in irrigation-induced cooling. *Proc. Nat. Acad. Sci.*, **104**, 13582–13587.

Brown, J. F., M. S. Pervez, and S. Maxwell, 2009: Mapping irrigated lands across the United States using MODIS satellite imagery. *Remote Sensing of Global Croplands for Food Security*, P. Thenkabail, J. G. Lyon, C. M. Biradar, and H. Turral, Eds., Taylor & Francis, 177–198.

Brown, J. F. and M. S. Pervez, 2014: Merging remote sensing data and national agricultural statistics to model change in irrigated agriculture. *Agricultural Systems*, **127**, 28–40.

Cook, B. L., M. J. Puma, and N. Y. Krakauer, 2011: Irrigation induced surface cooling in the context of modern and increased greenhouse gas forcing. *Clim. Dyn.*, **37**, 1587–1600.

Crook, N. A., 1996: Sensitivity of moist convection forced by boundary layer processes to low-level thermodynamic fields. *Mon. Wea. Rev.*, **124**, 1767–1785.

DeAngelis, A., F. Dominguez, Y. Fan, A. Robock, M. D. Kustu, and D. Robinson, 2010: Evidence of enhanced precipitation due to irrigation over the Great Plains of the United States. *J. Geophys. Res.*, **115**, D15115.

Earth System Research Laboratory, cited 2015: NCEP North American Regional Reanalysis. [Available online at http://www.esrl.noaa.gov/psd/data/gridded/data.narr.html].

Evans, J. P. and B. F. Zaitchik, 2008: Modeling the large-scale water balance impact of different irrigation systems. *Water Resour. Res.*, **44**, W08448.

Harding, K. J., and P. K. Snyder, 2012: Modeling the atmospheric response to irrigation in the Great Plains. Part I: General impacts on precipitation and the energy budget. *J. Hydrometeor.*,**13**, 1667–1686.

Hoerling, M., J. Eischeid, A. Kumar, R. Leung, A. Mariotti, K. Mo, S. Schubert, and R.

Seager, 2013: Causes and Predictability of the 2012 Great Plains Drought, *Bull Amer. Meteor. Soc.*, **95**, 269–282.

Irmak, S., 2010: Nebraska Water and Energy Flux Measurement, Modeling, and Research Network (NEBFLUX). *Trans. ASABE*, **53(4)**, 1097–1115.

Jones, C. A., and J. R. Kiniry, 1986: *CERES-Maize: A Simulation Model of Maize Growth and Development*. Texas A&M University Press, 194 pp.

King, M. D., S. E. Platnick, M. Wang, and K. Liou, 1997: Cloud Retrieval Algorithms for MODIS: Optical Thickness, Effective Particle Radius, and Thermodynamic Phase, *MODIS Algorithm Theoretical Basis Document. Version 5.*

King, M. D., and Coauthors, 2003: Cloud and aerosol properties, precipitable water and profiles of temperature and water vapor from MODIS. *IEEE Trans. Geosci. Remote Sensing*, **41**, 442–458.

Kropff, M. J., and H. H. van Laar, 1993: *Modelling Crop–Weed Interactions*. CABI, 274 pp.

Kueppers, L. M., M. A. Snyder, and L. C. Sloan, 2007: Irrigation cooling effect: Regional climate forcing by land-use change. *Geophysical Research Letters*, **34**, L03703.

Kueppers, L. M., and Coauthors, 2008: Seasonal temperature responses to land-use change in the western United States. *Global and Planetary Change*, **60**, 250–264.

Kueppers, L. M., and M. A. Snyder, 2011: Influence of irrigated agriculture on diurnal surface energy and water fluxes, surface climate, and atmospheric circulation in California. *Clim. Dyn.*, **38**, 1017-1029.

Lawrence, D.M., and Coauthors, 2011: Parameterization improvements and functional and structural advances in version 4 of the Community Land Model. *J. Adv. Model. Earth Sys.*, *3*.

Lawston, P. M., J. A. Santanello Jr., B. F. Zaitchik, M. Rodell, 2015: Impact of irrigation methods on land surface model spinup and initialization of WRF forecasts. *J. Hydrometeor.*, **16**, 1135–1154.

Lobell, D. B., C. Bonfils, J.M. Faurès, 2008: The role of irrigation expansion in past and future temperature trends. *Earth Interactions*, **12**, 1–11.

Mahmood, R., K.G. Hubbard, and C. Carlson, 2004: Modification of growing-season surface temperature records in the northern Great Plains due to land-use transformation: verification of modelling results and implication for global climate change, *International Journal of Climatology*, **24**, 311–327.

Maupin, M. A., J. F. Kenny, S. S. Hutson, J. K. Lovelace, N. L. Barber, and K. S. Linsey, Eds., 2014: *Estimated Use of Water in the United States in 2010.* Vol. 1405, 56 pp.

Maxwell, S. K., E. C. Wood, and A. Janus, 2008: Comparison of the USGS 2001 NLCD to the 2002 USDA Census of Agriculture for the Upper Midwest United States. *Agric. Ecosyst. Environ.*, **127**, 141–145.

Mesinger, F., and Coauthors, 2006: North American Regional Reanalysis. *Bull. Amer. Meteor. Soc.*, **87**, 343–360.

Myneni, R., 2012. *MODIS LAI/FPAR Product User's Guide.*

National Centers for Environmental Information (NCEI), cited 2016: Climatological Rankings. [Available online at http://www.ncdc.noaa.gov/temp-and-precip/climatological-rankings/.]

Oleson, K.W., and Coauthors 2010: Technical Description of version 4.0 of the Community Land Model (CLM). NCAR Technical Note NCAR/TN-478+STR, National Center for Atmospheric Research, Boulder, CO, 257 pp.

Ookouchi, Y., M. Segal, R. C. Kessler, and R. A. Pielke, 1984: Evaluation of soil moisture effects on the generation and modification of mesoscale circulations. *Mon. Wea. Rev.*, **112**, 2281–2292.

Pervez, M. S., and J. F. Brown, 2010: Mapping irrigated lands at 250-m scale by merging MODIS data and national agricultural statistics. *Remote Sensing*, **2**, 2388–2412.

Pielke, R. A., 2001: Influence of the spatial distribution of vegetation and soils on the prediction of cumulus Convective rainfall. *Rev. Geophys.*, **39**, 151–177.

Qian, Y., M. Huang, B. Yang, and L. K. Berg, 2013: A modeling study of irrigation effects on surface fluxes and land-air-cloud interactions in the southern Great Plains. *J. Hydrometeor.*, **14**, 700–721.

Raddatz, R. L., 2007: Evidence for the influence of agriculture on weather and climate through the transformation and management of vegetation: Illustrated by examples from the Canadian Prairies. *Agricultural and Forest Meteorology*, **142**, 186–202.

Segal, M., R. Avissar, M. C. McCumber, and R. A. Pielke, 1988: Evaluation of vegetation effects on the generation and modification of mesoscale circulations. *J. Atmos. Sci.*, **45**, 2268–2292.

Sellers, W. D., 1965: *Physical Climatology*, University of Chicago Press, 272 pp.

Siebert, S., P. Döll, J. Hoogeveen, J. M. Faures, K. Frenken, and S. Feick, 2005: Development and validation of the global map of irrigation areas. *Hydrol. Earth Syst. Sci.*, **9**, 535–547.

Siebert, S., J. Burke, J. M. Faures, K. Frenken, J. Hoogeveen, P. Döll, and F. T. Portmann, 2010: Groundwater use for irrigation – a global inventory. *Hydrol. Earth Syst. Sci.*, **14**, 1863–1880.

Skaggs, K. E., and S. Irmak, 2012: Long-term trends in air temperature distribution and extremes, growing degree-days, and spring and fall frosts for climate impact assessments on agricultural practices in Nebraska. *J. Appl. Meteorol. Clim.*, **142**, 2060–2073.

Skamarock, W. C., and Coauthors, 2008: A description of the Advanced Research WRF version 3. NCAR Tech. Note NCAR/TN-475+STR, 113 pp, doi:10.5065/D68S4MVH.

United States Department of Agriculture (USDA), 2004: 2002 census of agriculture: Farm and ranch irrigation survey (2003), Vol. 3, Special Studies, Part 1, USDA Tech. Rep., NTIS AC-02-SS-1, 216 pp.

United States Department of Agriculture (USDA), 2014: 2012 census of agriculture: Farm and ranch irrigation survey (2013), Vol. 3, Special Studies, Part 1, USDA Tech. Rep., NTIS AC-12-SS-1, 266 pp.

United States Geological Survey (USGS), cited 2016: Global Land Cover Characterization. [Available online at http://edc2.usgs.gov/glcc/background.php.]

Wan, Z., 1999: *MODIS Land-Surface Temperature Algorithm Theoretical Basis Document (LST ATBD). Version 3.3.*

Wan, Z., 2009: *Collection-5 MODIS Land Surface Temperature Products Users' Guide.*

Wang, J., A. L. Kessner, C. Aegerter, A. Sharma, L. Judd, B. Wardlow, J. You, M. Shulski, S. Irmak, and A. Kilic, 2015: A multi-sensor view of the 2012 Central Plains drought from space. *Frontiers in Environmental Science*, **4:45**, 13 pp.

Wardlow, B. and K. Callahan, 2014: A multi-scale accuracy assessment of the MODIS irrigated agriculture data-set (MIrAD) for the state of Nebraska, USA. *GIScience & Remote Sensing*, **51**, 572–592.

Yang, H. S., A. Dobermann, J. L. Lindquist, D. T. Walters, T. J. Arkebauer, and K. G. Cassman, 2004: Hybrid-maize—a maize simulation model that combines two crop modeling approaches. *Field Crops Research*, **87**, 131–154.

Zaitchik, B. F., J. Evans, and R. B. Smith, 2005: MODIS-derived boundary conditions for

a mesoscale climate model: Application to irrigated agriculture in the Euphrates basin. *Mon. Wea. Rev.*, **133**, 1727–1743.

Tables

Table 1. MODIS products used in this study.

Product	Satellite Sensor	Temporal Resolution	Spatial Resolution	Citation
MOD11C3: Land Surface Temperature	Terra MODIS	Monthly	0.05°	Wan 1999; Wan 2009
MOD08_M3: Cloud Fraction	Terra MODIS	Monthly	1°	King et al. 2003
MOD06L2: Cloud Fraction	Terra MODIS	Daily	5 km	King et al. 1997
MOD15A2: Leaf Area Index	Terra MODIS	8 days	1 km	Knyazikhin et al. 2012

Table 2. Configuration of WRF and physics schemes used.

WRF Version	3.6.1
Resolution	12 km
Boundary Conditions	North American Regional Reanalysis
Land Surface Model	Community Land Model 4.0
Microphysics	WRF Single-Moment 3-Class Scheme
Longwave Radiation	Rapid Radiative Transfer Model
Shortwave Radiation	Dudhia Scheme
Planetary Boundary Layer	Yonsei University Scheme
Cumulus Parameterization	Kain-Fritsch Scheme

Table 3. WRF runs in the sensitivity experiment.

Run Name	Land-Use	Soil Moisture	Leaf Area Index
WRF-DF	Default	Default	Default
WRF-DF-50S	Default	Increase to 50% if < 50%	Default
WRF-Ctrl	MIrAD	Default	Default
WRF-DS-HLAI	MIrAD	Default	Hybrid Maize
WRF-50S-DLAI	MIrAD	Increase to 50% if < 50%	Default
WRF-50S-HLAI	MIrAD	Increase to 50% if < 50%	Hybrid Maize
WRF-NoIrri	NE irrigated cropland becomes Grassland	Default	Default

Table 4. Average simulated T_{2m} error (K) with respect to AWDN observations.

	Local Time (CDT)								
Run Name	**1:00**	**4:00**	**7:00**	**10:00**	**13:00**	**16:00**	**19:00**	**22:00**	**Land-Use**
	2.55	2.33	0.92	2.99	4.53	4.96	5.55	2.96	All
WRF-Ctrl	2.89	2.64	1.19	3.41	5.07	5.56	6.17	3.30	Irrigated
	2.25	2.17	1.05	3.32	5.05	5.39	5.42	2.47	Dryland
	2.65	2.42	1.01	3.06	4.59	4.99	5.60	3.06	All
WRF-DS-HLAI	2.84	2.59	1.17	3.41	5.12	5.56	6.15	3.22	Irrigated
	2.67	2.52	1.33	3.50	5.15	5.47	5.63	2.91	Dryland
	1.86	1.73	0.43	2.17	3.88	4.39	4.70	2.16	All
WRF-50S-DLAI	1.47	1.43	0.21	1.63	3.80	4.55	4.34	1.63	Irrigated
	2.14	2.04	0.93	3.29	4.91	5.14	5.38	2.37	Dryland
	1.88	1.78	0.45	2.08	3.69	4.27	4.49	2.19	All
WRF-50S-HLAI	1.39	1.42	0.18	1.46	3.43	4.28	3.83	1.52	Irrigated
	2.33	2.23	1.02	3.22	4.81	5.16	5.39	2.60	Dryland

Figures

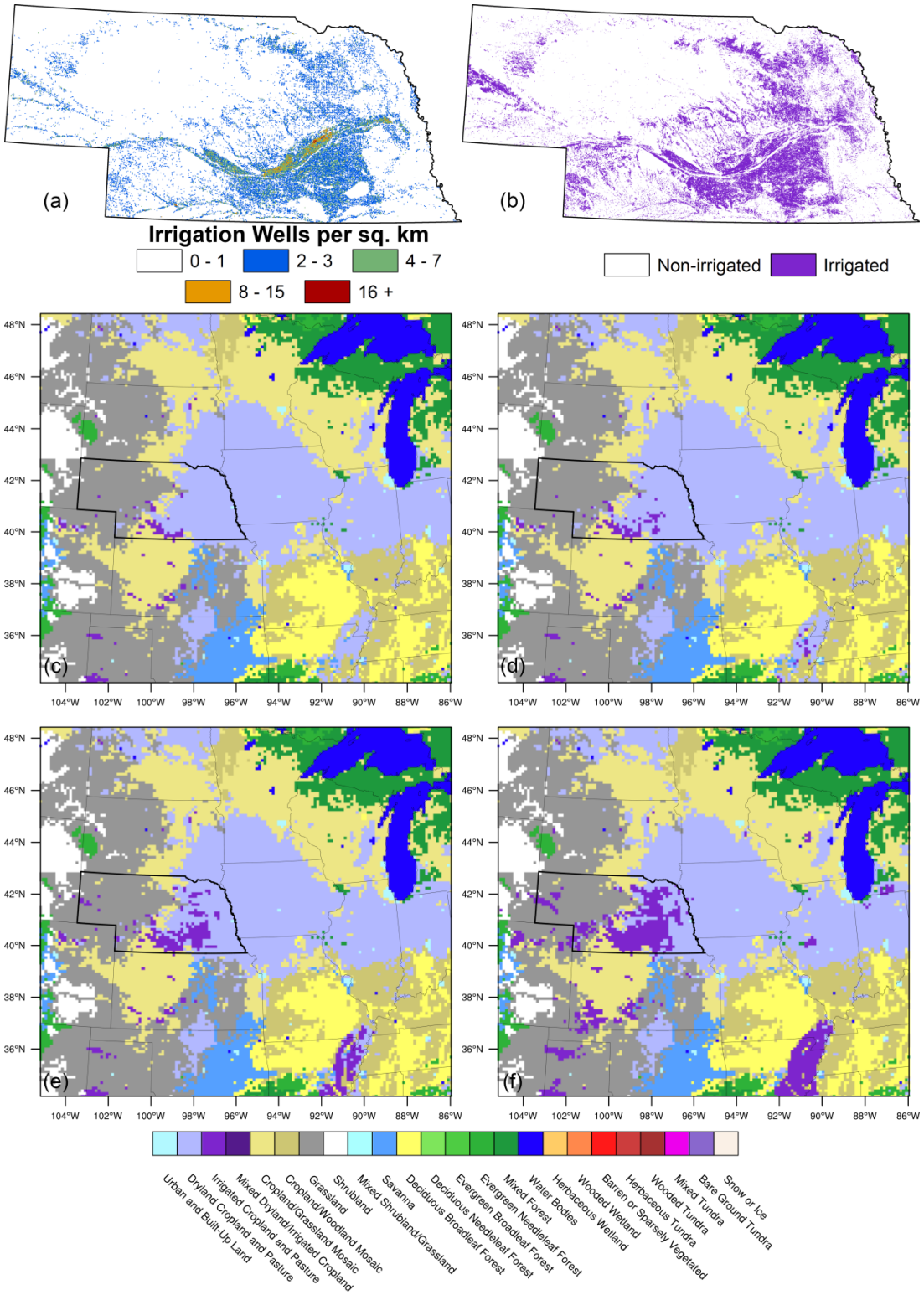

Figure 1. (a) Density of registered irrigation wells in Nebraska (per square kilometer), (b)

MODIS irrigated agriculture dataset (MIrAD) for Nebraska, and (c) WRF default land-use dataset. (d), (e), and (f) are land-use datasets using 75%, 50%, and 25% thresholds, respectively, for classification of WRF land-use as “irrigated cropland and pasture” (e.g. for the 75% threshold, 75% of the MIrAD pixels within a single WRF pixel must be classified as “irrigated” for the WRF pixel to be classified as “irrigated cropland and pasture”).

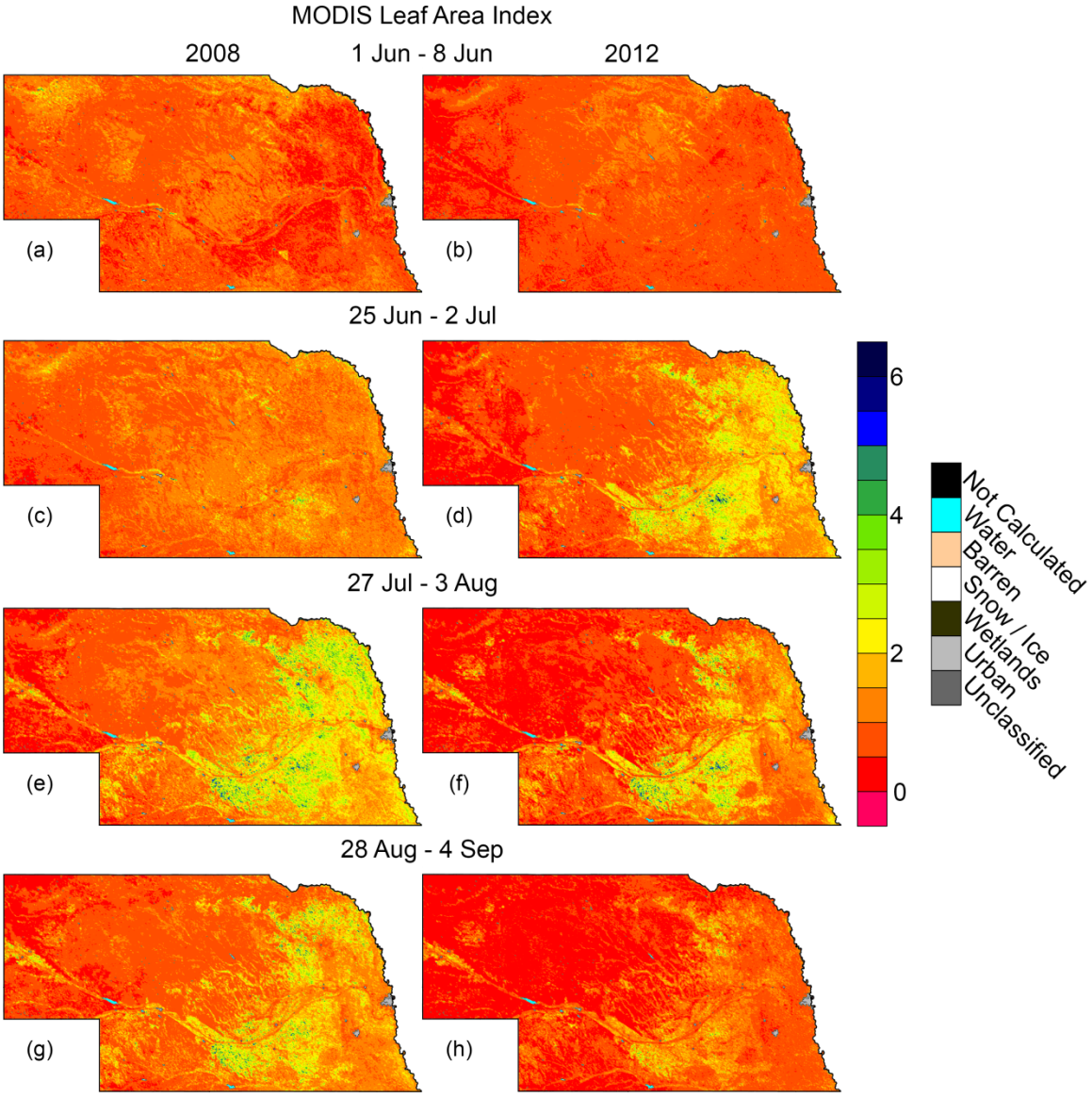

Figure 2. 8-day average leaf area index from MODIS aboard Terra for summer of 2008 (left column) and summer of 2012 (right column). 2008 is a “normal” precipitation year in Nebraska.

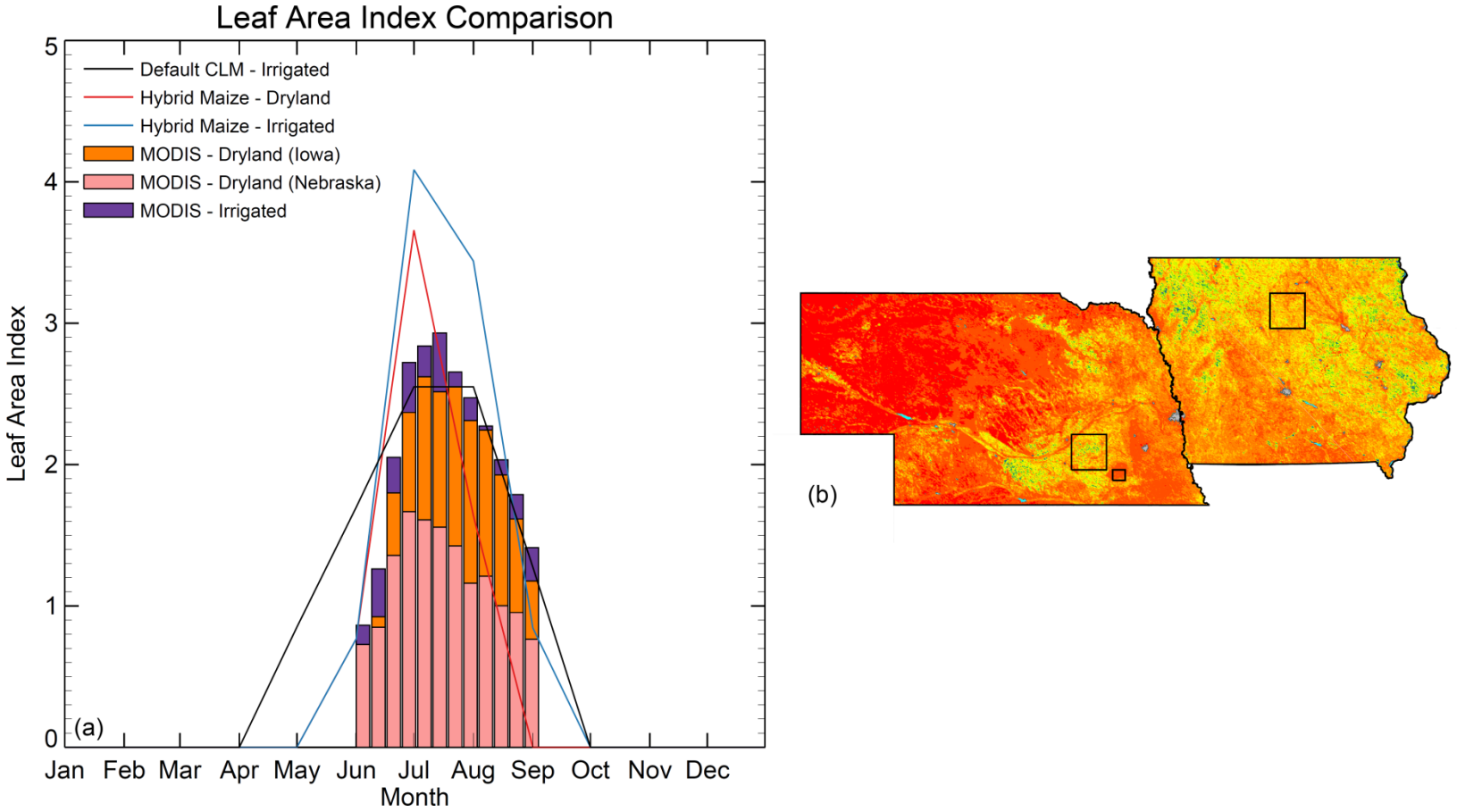

Figure 3. (a) Comparison of several modeled/MODIS-derived leaf area index values. Default input irrigated and dryland cropland leaf area index used in CLM (black line), Hybrid Maize crop model simulation irrigated leaf area index for summer 2012 (solid blue line), Hybrid Maize crop model simulation irrigated leaf area index for summer 2012 as used in CLM (dashed blue line), Hybrid Maize crop model simulation dryland leaf area index for summer 2012 (solid red line), Hybrid Maize crop model simulation dryland leaf area index for summer 2012 as used in CLM (dashed red line), MODIS irrigated 8-day average leaf area index for summer 2012 (purple

bars), MODIS dryland (Iowa) 8-day average leaf area index for summer 2012 (orange bars), and MODIS dryland (Nebraska) 8-day average leaf area index for summer 2012 (pink bars). (b) shows areas representing irrigated (large box) and dryland (small box) in Nebraska, as well as a dryland area in Iowa.

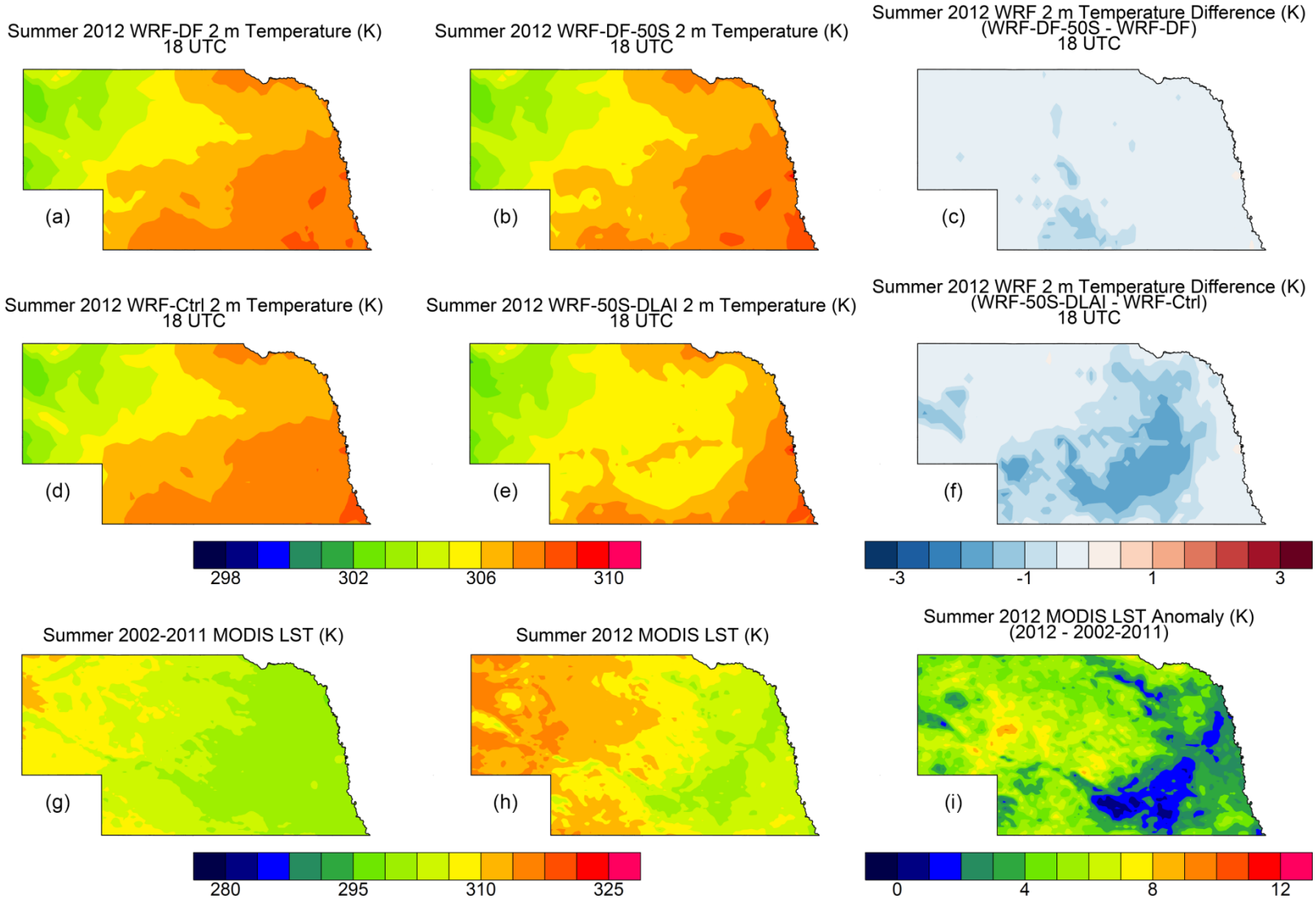

Figure 4. Simulated summer 2012 2 m temperature averaged at 18 UTC in Nebraska for (a) WRF-DF and (b) WRF-DF-50S. (c)

WRF-DF-50S and WRF-DF 2 m temperature difference for summer 2012 at 18 UTC ((b) minus (a)). (d), (e), and (f) as in (a), (b), and (c), but for WRF-Ctrl and WRF-50S-DLAI. (g) Summer 2002-2011 average land surface temperature, (h) summer 2012 average land surface temperature, and (i) summer 2012 land surface temperature anomaly ((h) minus (g)) from Terra MODIS. Note different scales are applied to the color bar for T_{2m} and LST.

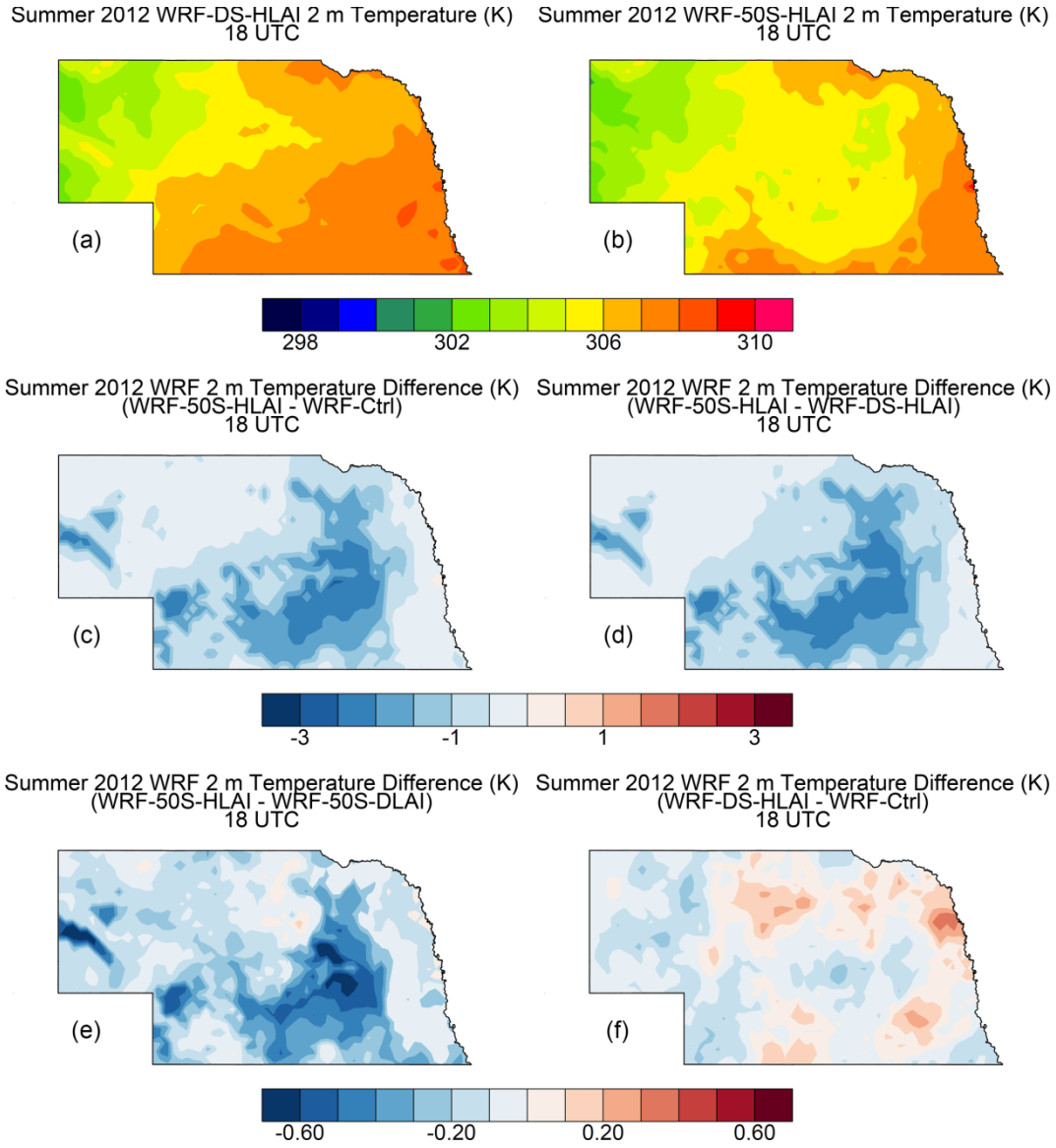

Figure 5. Simulated summer 2012 2 m temperature averaged at 18 UTC in Nebraska for (a) WRF-DS-HLAI and (b) WRF-50S-HLAI. Simulated summer 2012 2 m temperature difference averaged at 18 UTC for (c) WRF-50S-HLAI and WRF-Ctrl, (d) WRF-50S-HLAI and WRF-DS-HLAI, (e) WRF-50S-HLAI and WRF-50S-DLAI, and (f) WRF-DS-HLAI and WRF-50S-CTRL. Note different scales are applied to the color bars for (c) and (d) vs. (e) and (f).

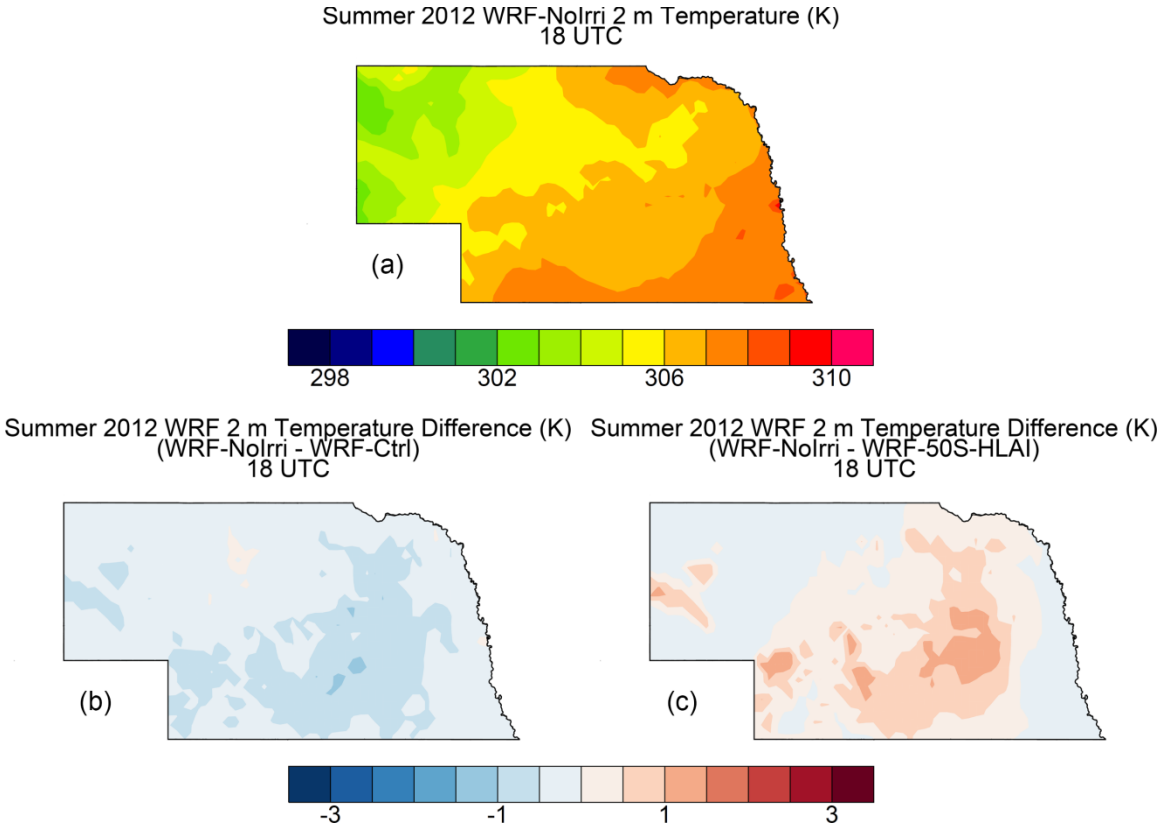

Figure 6. (a) Simulated summer 2012 2 m temperature averaged at 18 UTC in Nebraska for WRF-NoIrri. Simulated summer 2 m temperature difference averaged at 18 UTC for WRF-NoIrri and (b) WRF-Ctrl and (c) WRF-50S-HLAI.

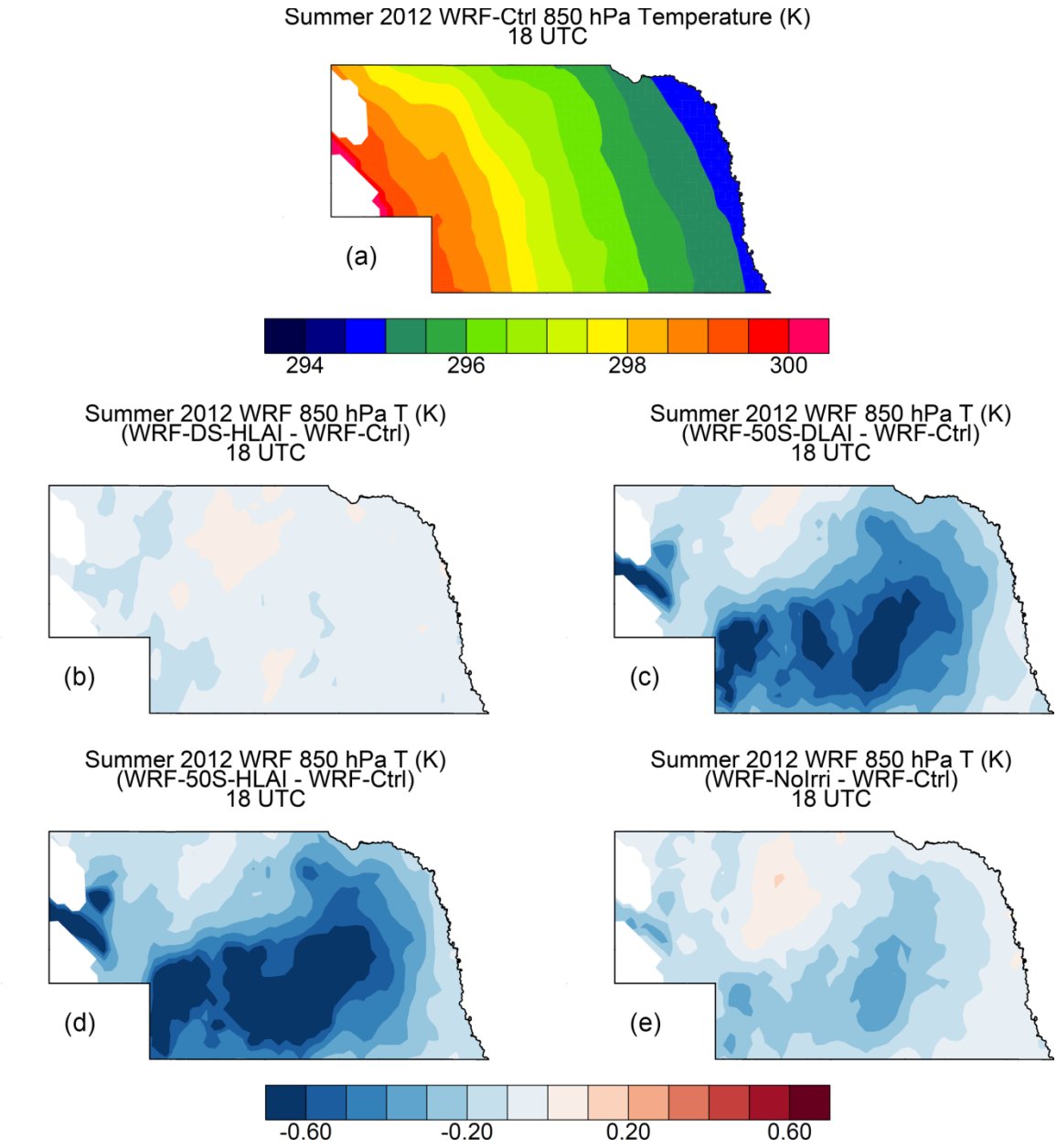

Figure 7. (a) Simulated summer 2012 850 hPa temperature averaged at 18 UTC for WRF-Ctrl. Simulated summer 2012 850 hPa temperature difference vs. WRF-Ctrl averaged at 18 UTC for (b) WRF-DS-HLAI, (c) WRF-50S-DLAI, (d) WRF-50S-HLAI, and (e) WRF-NoIrri. Note areas in which surface pressure is less than 850 hPa are not plotted.

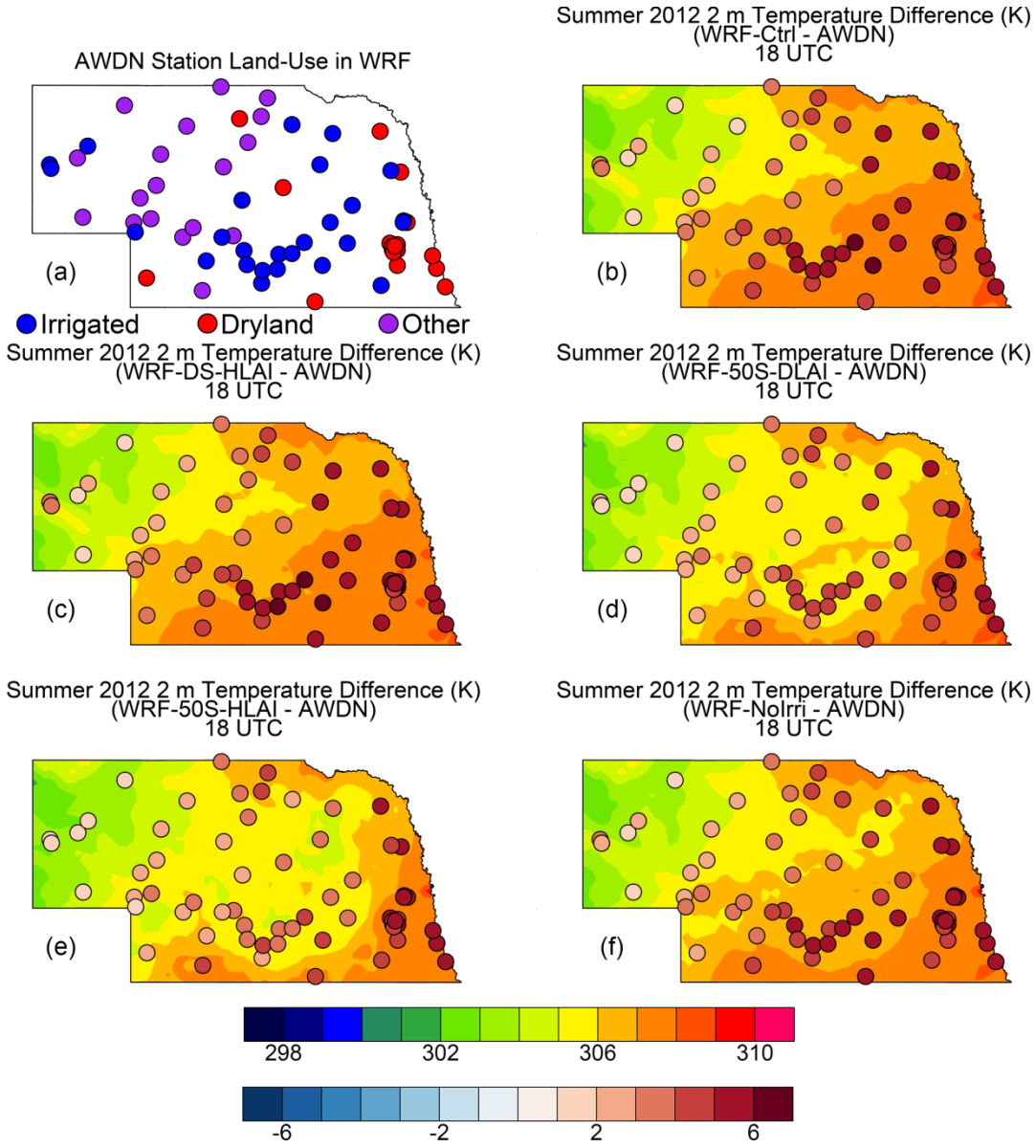

Figure 8. (a) Land-use classification of AWDN stations. AWDN observed and simulated summer 2012 2 m temperature difference averaged at 18 UTC for (b) WRF-Ctrl, (c) WRF-DS-HLAI, (d) WRF-50S-DLAI, (e) WRF-50S-HLAI, and (f) WRF-NoIrri overlaid on simulated summer 2012 2 m temperature averaged at 18 UTC for each respective WRF run.

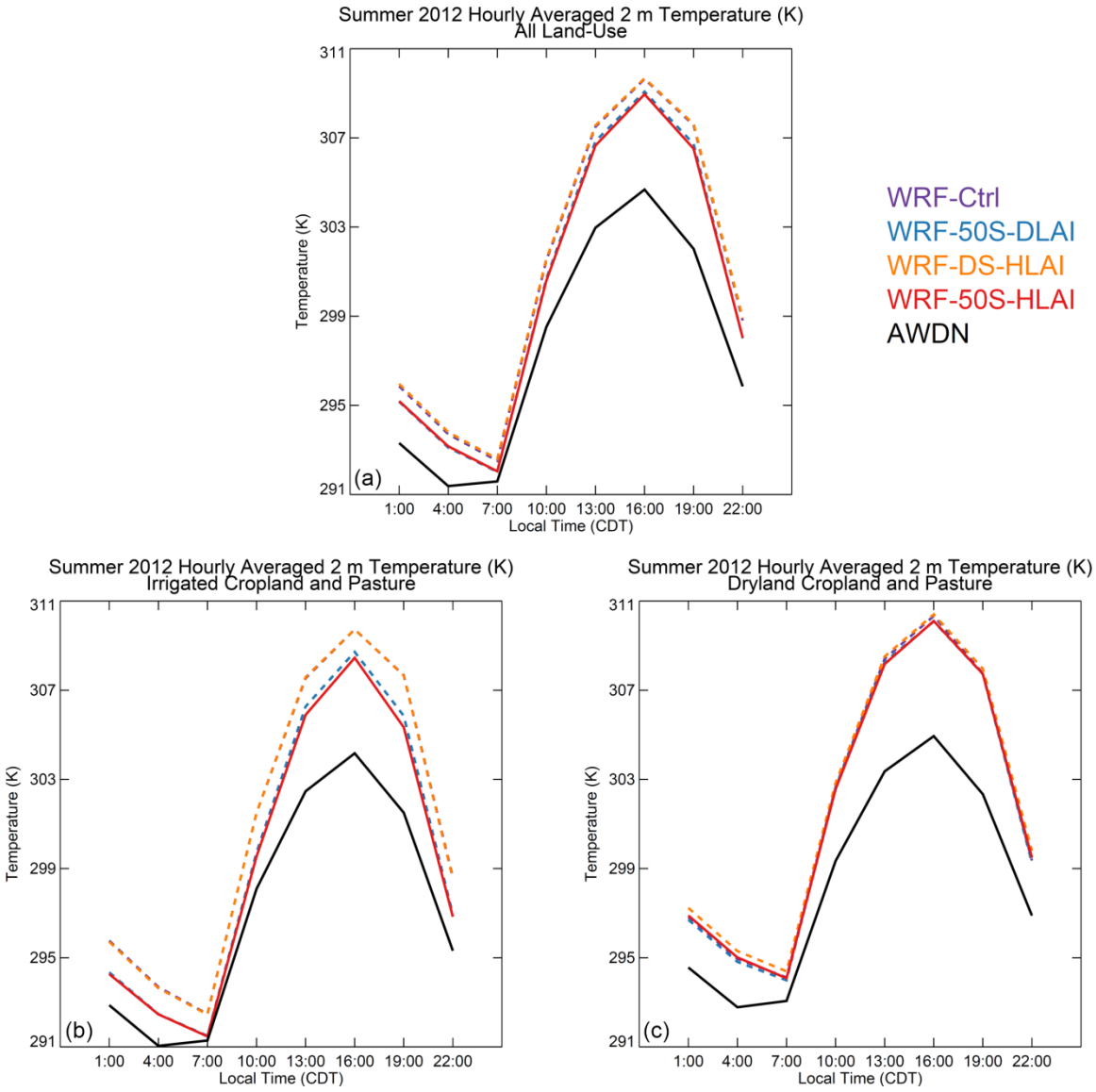

Figure 9. Hourly averaged 2 m temperature in Nebraska for (a) all land-uses, (b) irrigated cropland and pasture, and (c) dryland cropland and pasture for WRF-Ctrl (purple dashed line), WRF-50S-DLAI (blue dashed line), WRF-DS-HLAI (orange dashed line), WRF-50S-HLAI (red solid line), and AWDN observations (black solid line).

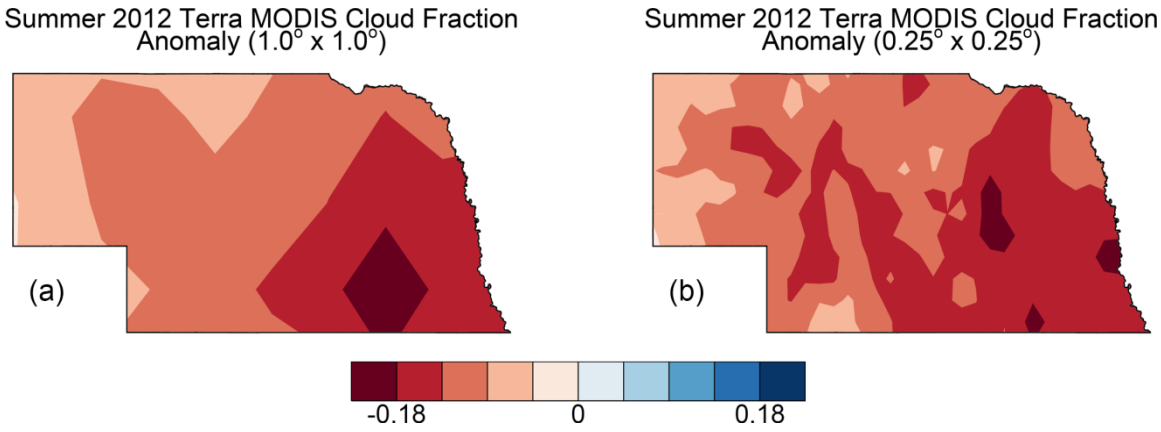

Figure 10. Summer 2012 cloud fraction anomaly from (a) MODIS level 3 monthly data and (b) MODIS level 2 granules re-gridded to 0.25°×0.25°.

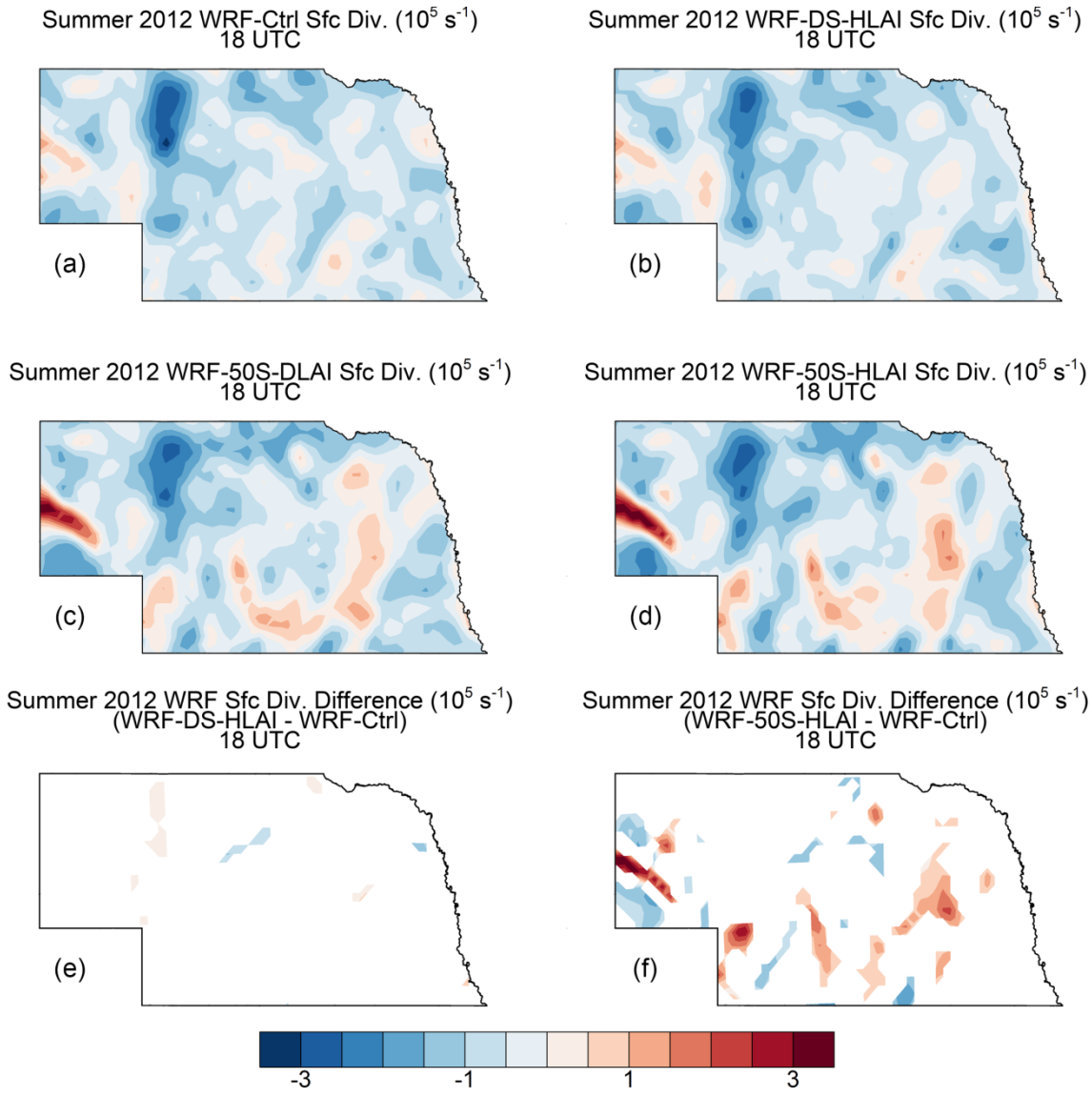

Figure 11. Simulated summer 2012 surface divergence averaged at 18 UTC in Nebraska for (a) WRF-Ctrl, (b) WRF-DS-HLAI, (c) WRF-50S-DLAI, and (d) WRF-50S-HLAI. Simulated summer 2012 surface divergence difference vs. WRF-Ctrl averaged at 18 UTC for (e) WRF-DS-HLAI, and (f) WRF-50S-HLAI. Areas plotted in (e) and (f) are those found to be statistically significant at a 95% confidence level using a two-tailed, paired *t* test.

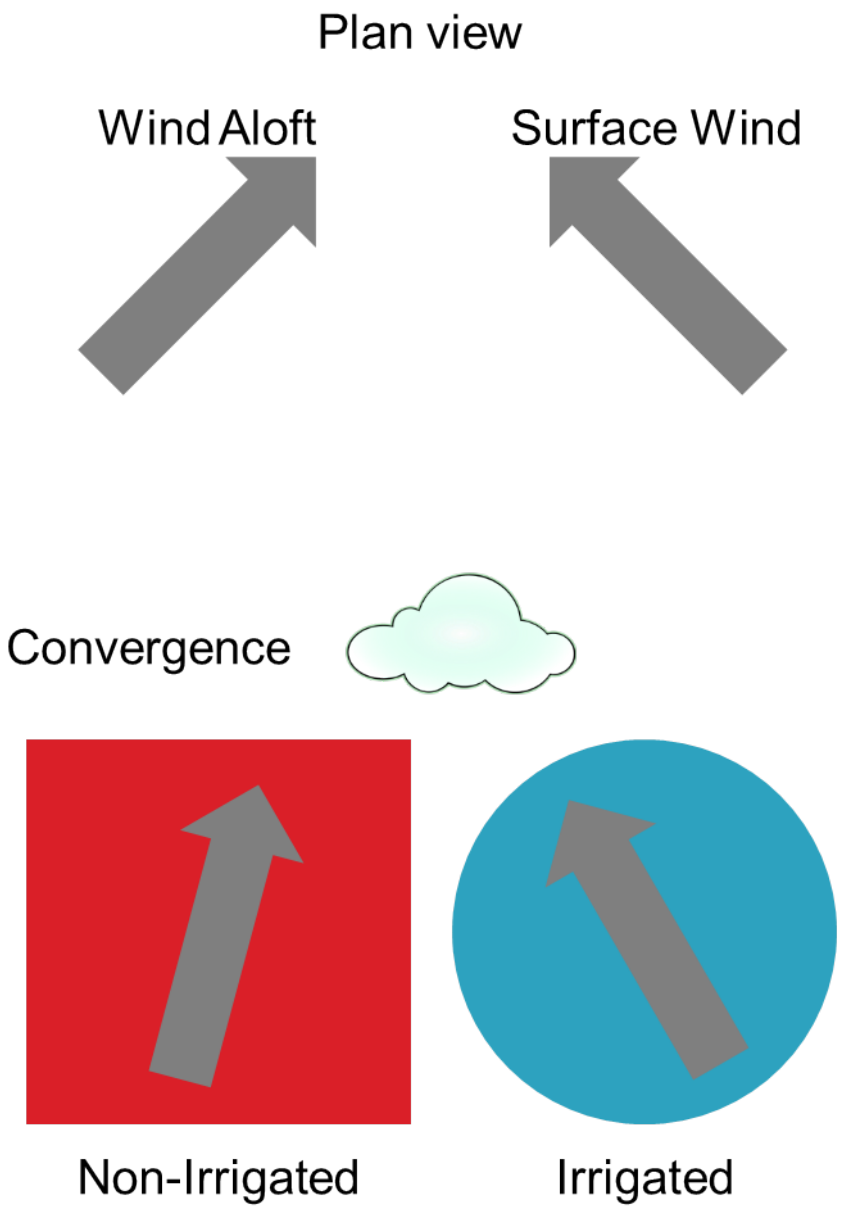

Figure 12. Plan view of hypothesis that wind over irrigated areas will have a wind direction closer to that of the surface while wind over non-irrigated areas will have a wind direction closer to that of the winds aloft.

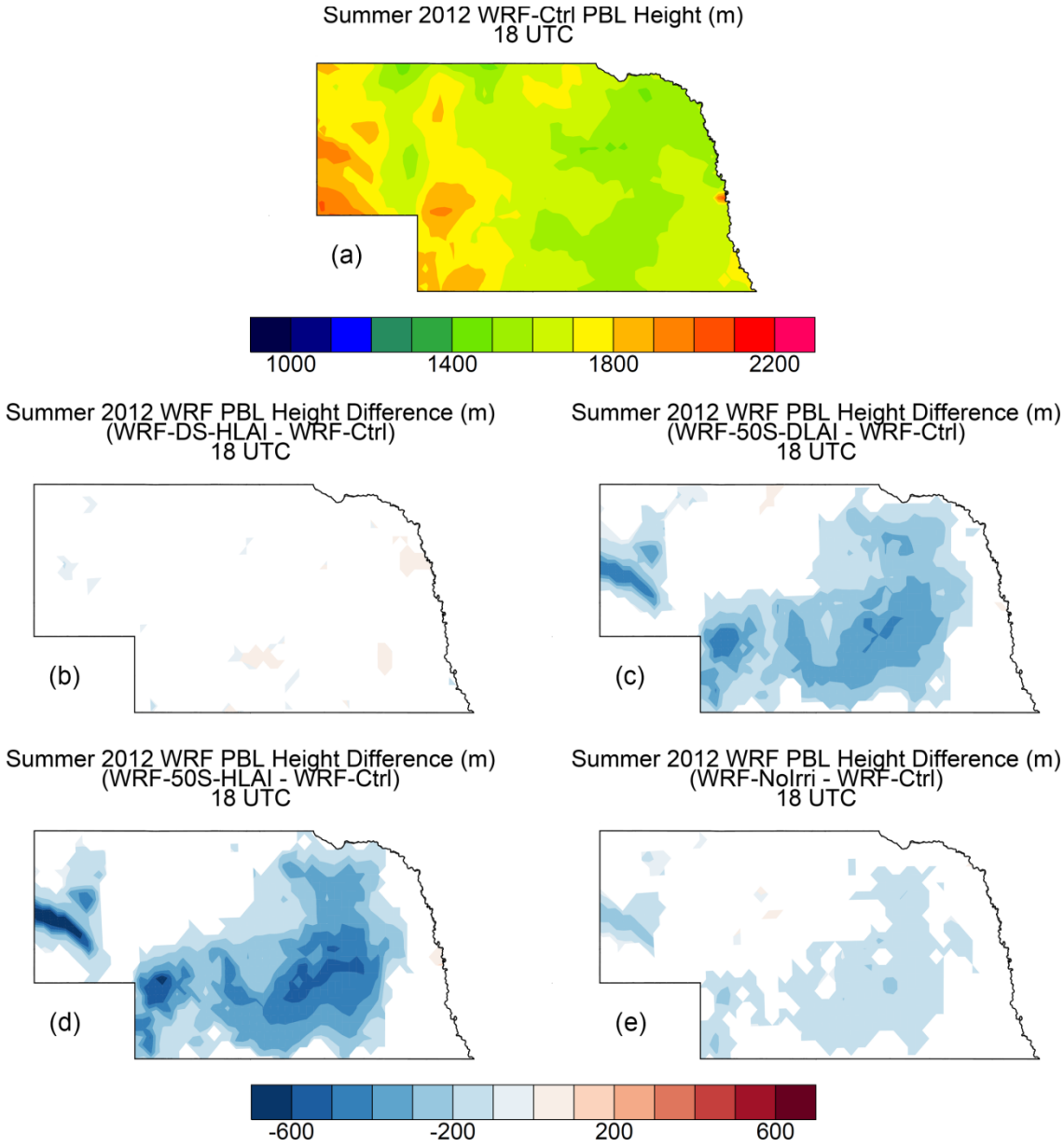

Figure 13. (a) Simulated summer 2012 planetary boundary layer height averaged at 18 UTC for WRF-Ctrl. Simulated summer 2012 planetary boundary layer height difference vs. WRF-Ctrl averaged at 18 UTC for (b) WRF-DS-HLAI, (c) WRF-50S-DLAI, (d) WRF-50S-HLAI, and (e) WRF-NoIrri. Areas plotted are those found to be statistically significant at a 95% confidence level using a two-tailed, paired *t* test.

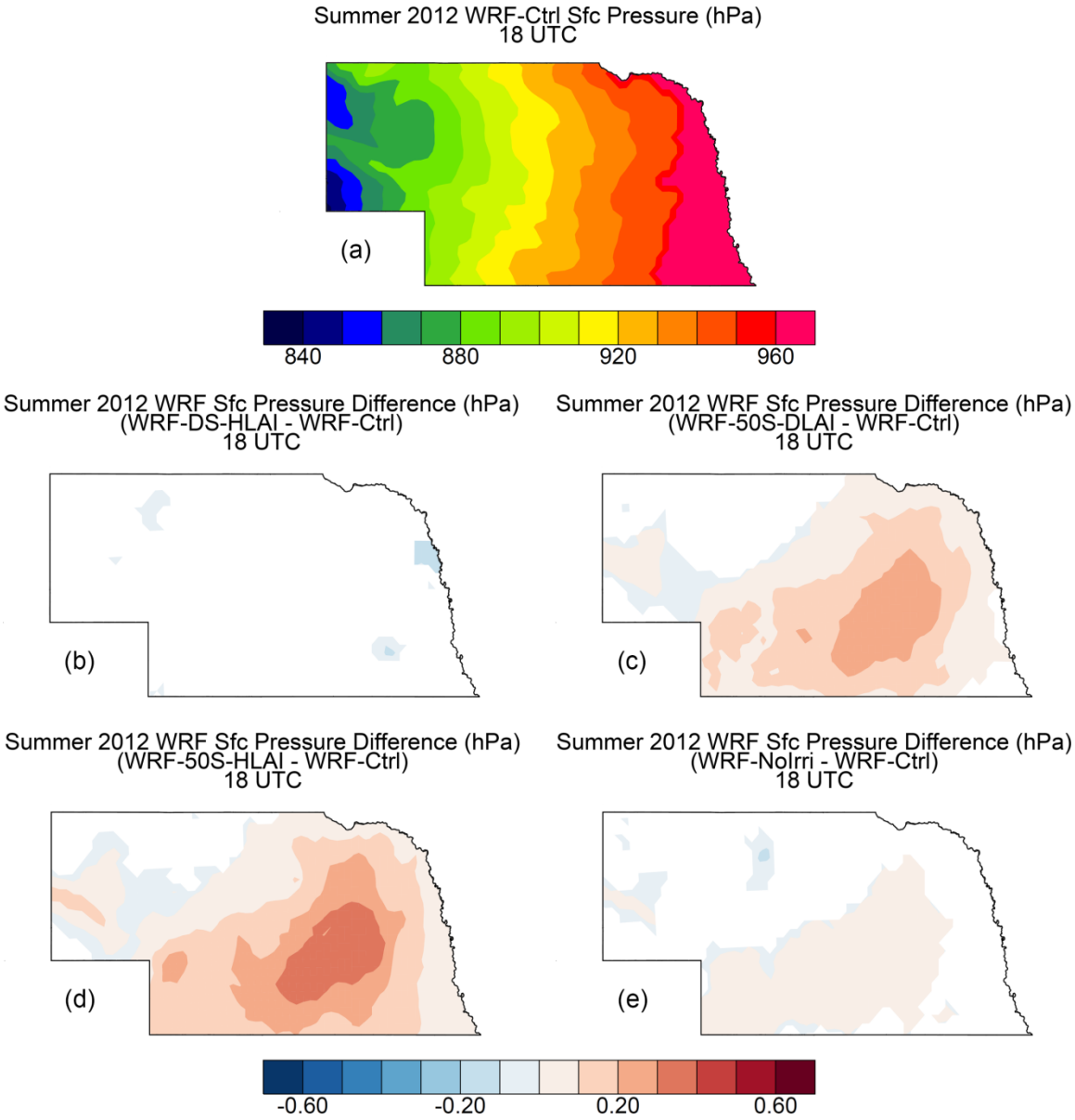

Figure 14. (a) Simulated summer 2012 surface pressure averaged at 18 UTC for WRF-Ctrl. Simulated summer 2012 surface pressure difference vs. WRF-Ctrl averaged at 18 UTC for (b) WRF-DS-HLAI, (c) WRF-50S-DLAI, (d) WRF-50S-HLAI, and (e) WRF-NoIrri. Areas plotted are those found to be statistically significant at a 95% confidence level using a two-tailed, paired *t* test.